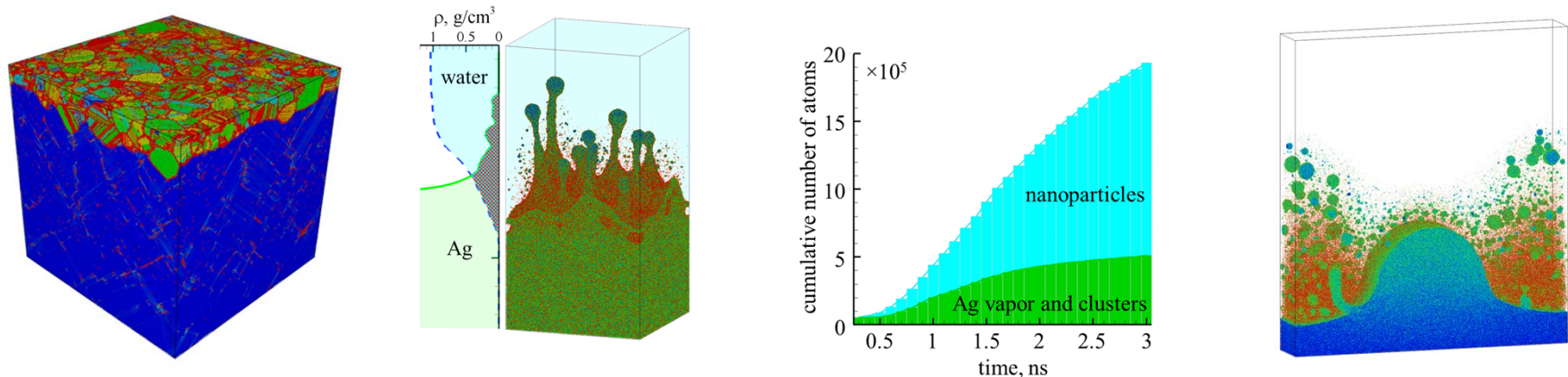


Atomistic simulations of nanoparticle generation by short pulse laser ablation of AgCu bilayers in liquid

Cheng-Yu Shih, Chaobo Chen, Maxim Shugaev, Hao Huang, Leonid Zhigilei

University of Virginia, Department of Materials Science and Engineering



Collaborators:

Bilal Gökce and **Stephan Barcikowski**, University of Duisburg-Essen, Germany

Wolfgang Kautek, University of Vienna, Austria

Iaroslav Gnilitskyi, NoviNano Lab LLC, Lviv, Ukraine

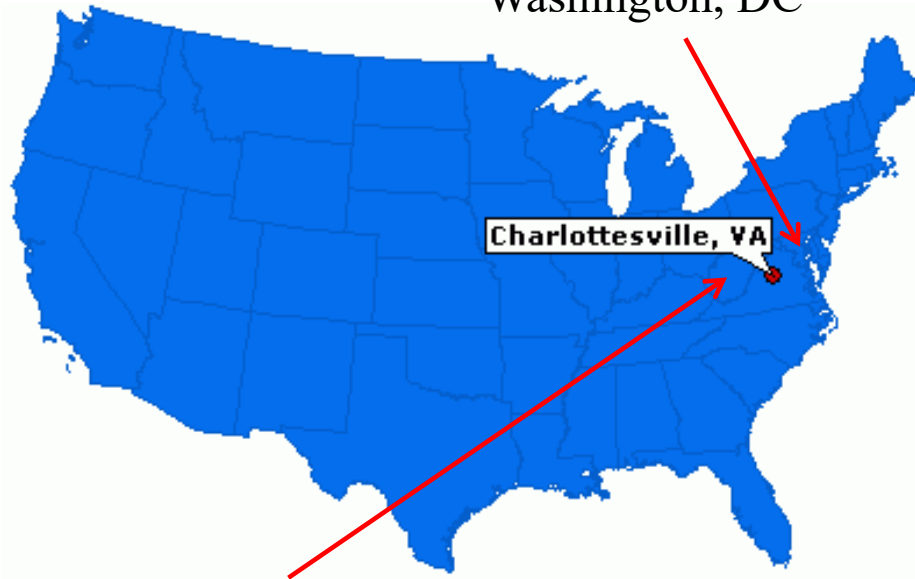
Emmanuel Stratakis, University of Crete, Heraklion, Greece

Funding support: NSF (DMR-1610936 and CMMI-1663429)

Computational support: OLCF at ORNL (project MAT130), XSEDE (project TG-DMR110090)

University of Virginia

Washington, DC



Charlottesville, VA

Appalachian Mountains



Founded by Thomas Jefferson in 1819
~22,000 students, ~2000 academic staff

- College of Arts & Sciences
- School of Engineering & Applied Science
- School of Architecture
- Darden School of Business
- McIntire School of Commerce
- Curry School of Education
- School of Law
- School of Medicine

Graduate programs at UVa Engineering



Monthly news letters with information about fellowships and travel grant opportunities, events, seminars, BBQ or beer parties organized by Graduate Student Board, *etc.*

All graduate students get stipend (~\$26K/year) + health insurance; time to PhD is 3-6 years
Can apply after M.S. or B.S. degrees.

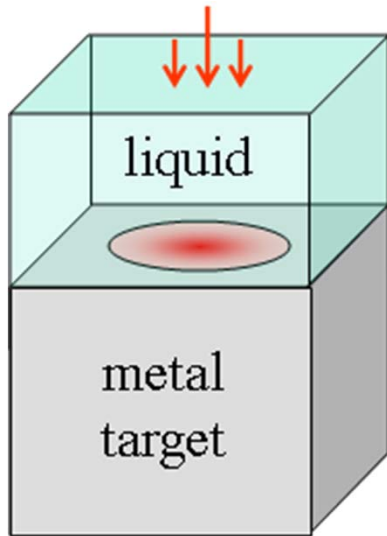
Materials Science and Engineering Department:

Strength in Electrochemistry/Corrosion, Physical Metallurgy (phase transformations, crystal defects, alloys), Advanced Material Characterization (TEM/FIB, SEM, STM, ...);

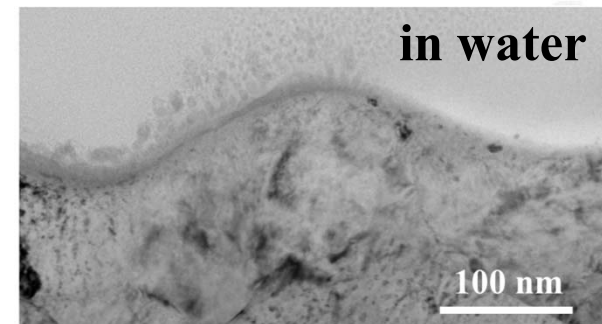
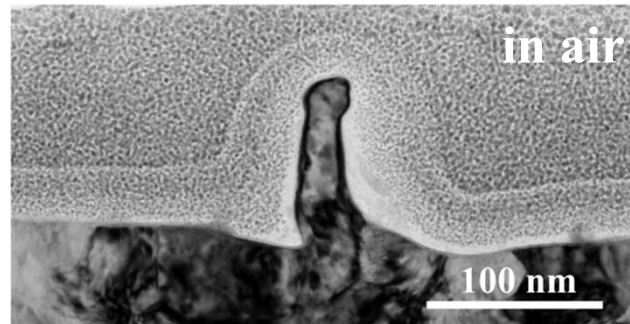
New hires/emerging strength in Additive Manufacturing, Materials Informatics, Soft Matter.

Interested to learn more? Do not hesitate to contact me!

Effect of liquid confinement on surface modification



surface micro/nano-structuring by laser processing in liquids
mechanical confinement + additional cooling channel →
nonequilibrium microstructure & smoothing of surface morphology

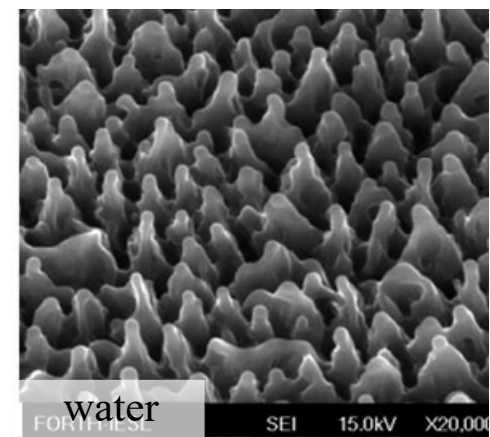
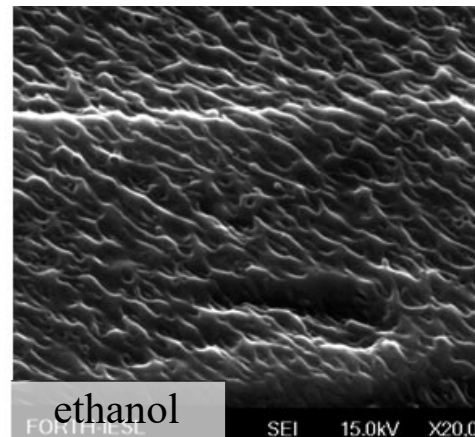


Surface features produced by single shot ablation of Cr (001) target irradiated at 6000 J/m^2 incident laser fluence in air and water
Shih, Gnilitzkyi, Shugaev, Skoulas, Stratakis, and Zhigilei, *Nanoscale* **12**, 7674, 2020

Type of the liquid plays a role

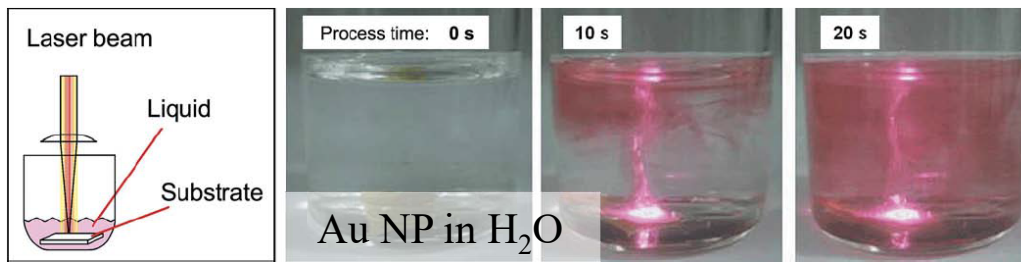
5 ps laser processing of Ti in ethanol and water

Barmina *et al.*,
Quant. Electron. **40**, 1012, 2010



Laser ablation in liquids for synthesis of nanoparticles

synthesis of clean colloidal nanoparticles with unique shapes and functionalities

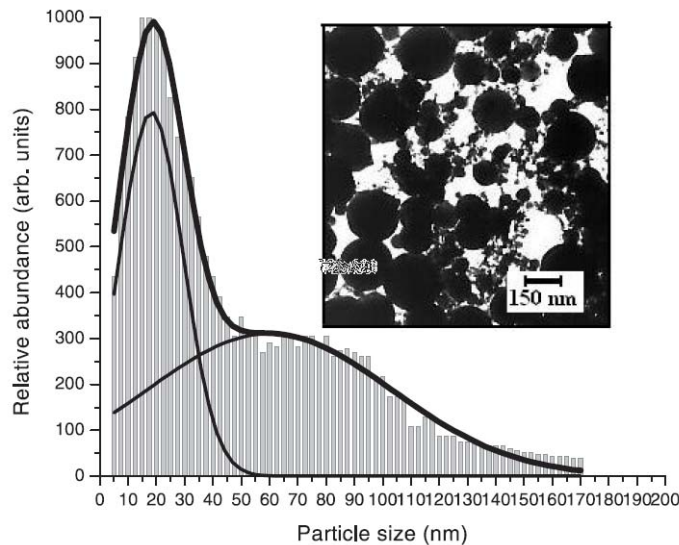


Wagener *et al.*, *Photonik Int.* 20, 2011

clean NPs for biomedicine, catalysis, plasmonics, *etc.*

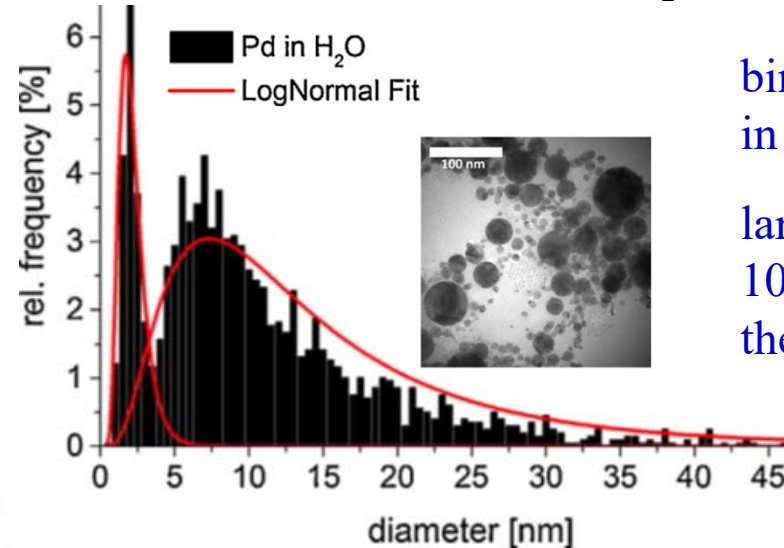
size, structure and composition of NPs can be controlled by T , viscosity of liquid medium, surfactants, PLFL, *etc.*

120 fs laser ablation of Au in H₂O



Sylvestre *et al.*, *Appl. Phys. A* **80**, 758, 2005

9.8 ps laser ablation of Pd in H₂O

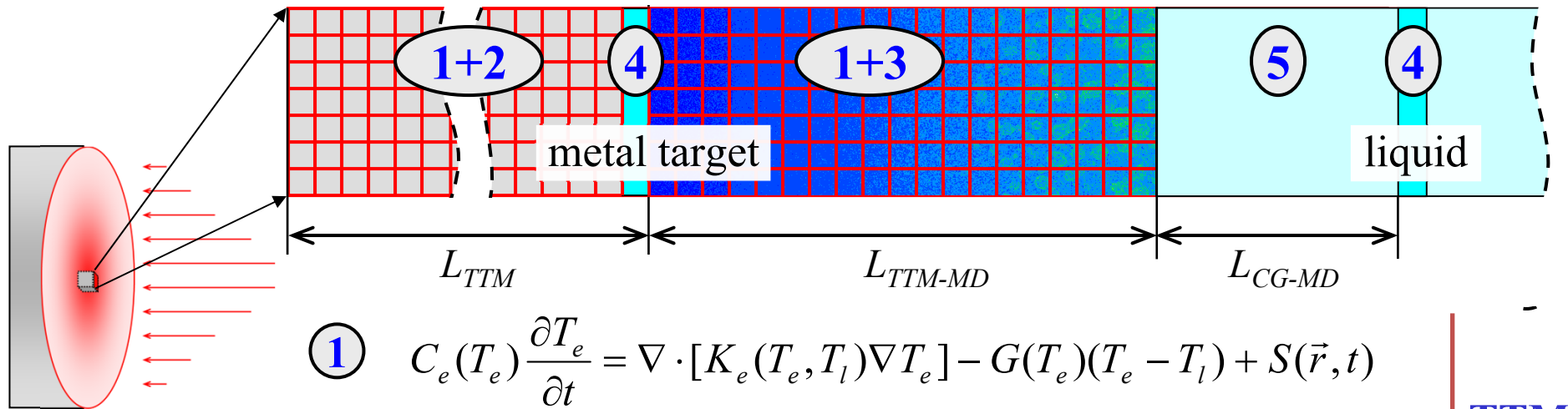


bimodal size distribution in fs and ps PLAL

large (several 10s to 100s of nm) dominate the mass concentration

Marzun *et al.*, *Appl. Surf. Sci.* **348**, 75, 2015

TTM-MD model for laser interaction with metals in liquid environment



$$\textcircled{1} \quad C_e(T_e) \frac{\partial T_e}{\partial t} = \nabla \cdot [K_e(T_e, T_l) \nabla T_e] - G(T_e)(T_e - T_l) + S(\vec{r}, t)$$

$$\textcircled{2} \quad C_l(T_l) \frac{\partial T_l}{\partial t} = \nabla \cdot [K_l(T_l) \nabla T_l] + G(T_e)(T_e - T_l)$$

$$\textcircled{3} \quad m_i \frac{d^2 \vec{r}_i}{dt^2} = \vec{F}_i + \zeta m_i \vec{v}_i^{th}, \quad T_l^{cell} = \sum_{cell} m_i (v_i^{th})^2 / (3k_B N_{cell})$$

$\textcircled{4}$ pressure-transmitting boundary conditions

$\textcircled{5}$ coarse-grained MD representation of liquid environment

TTM

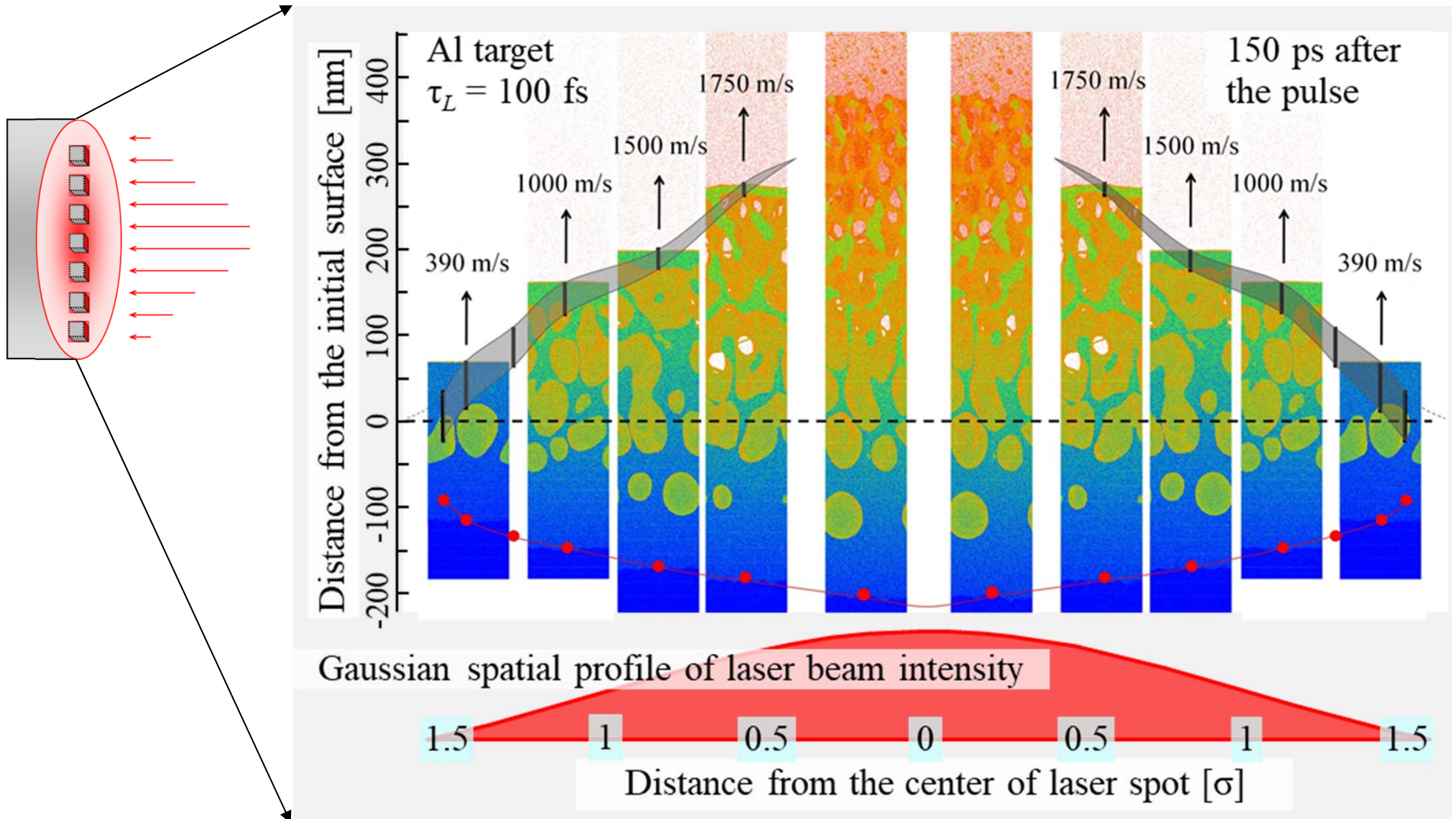
MD

TTM-MD model: MD is combined with TTM to account for (1) laser energy absorption by conduction band electrons, (2) electron-phonon equilibration, (3) electronic heat conduction

Coarse-grained model for liquids: heat bath approach accounts for missing degrees of freedom

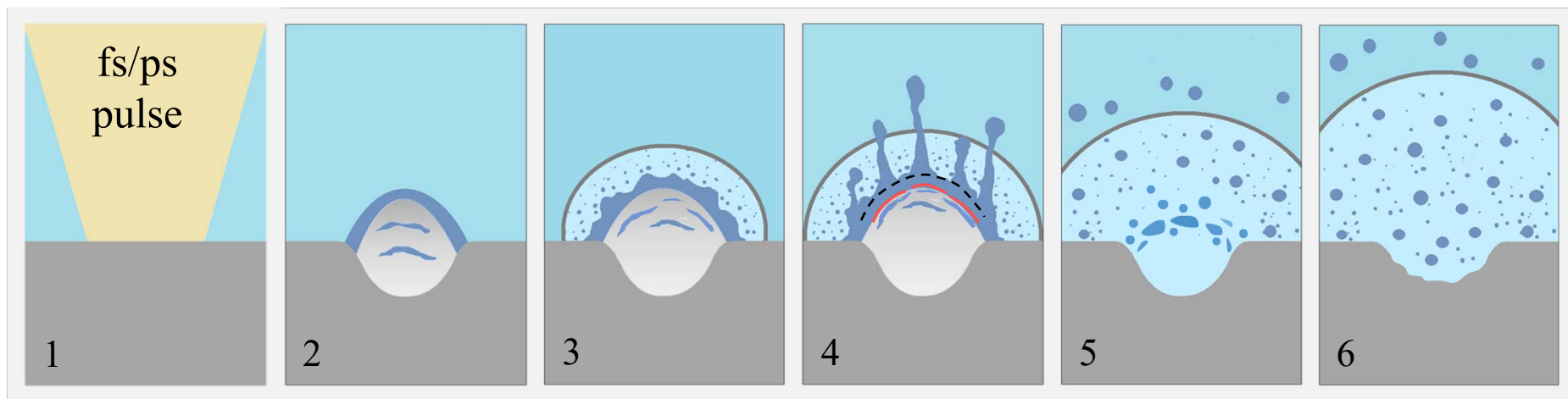
Acoustic impedance matching boundary conditions: nonreflective propagation of stress waves

“mosaic” approach to mapping processes occurring at the scale of the whole laser spot



Wu and Zhigilei, *Appl. Phys. A* **114**, 11, 2014.
Shugaev *et al.*, *MRS Bull.* **41**, 960, 2016.

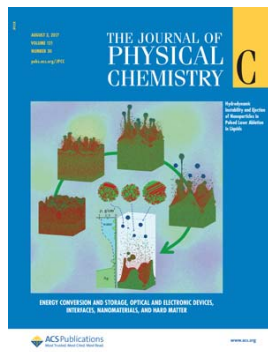
Summary on short (fs/ps) pulse laser ablation in liquids



Two mechanisms of NP generation in fs/ps PLAL:

1. Rapid nucleation & growth in water-metal mixing region → **small (≤ 10 nm) NPs**
2. Rayleigh-Taylor and Richtmyer-Meshkov instabilities at interface between superheated metal layer and water → **large (10s of nm) NPs**

Rapid quenching (10^{12} K/s) → NPs with complex microstructure and, possibly, **nonequilibrium/metastable** phases/structures



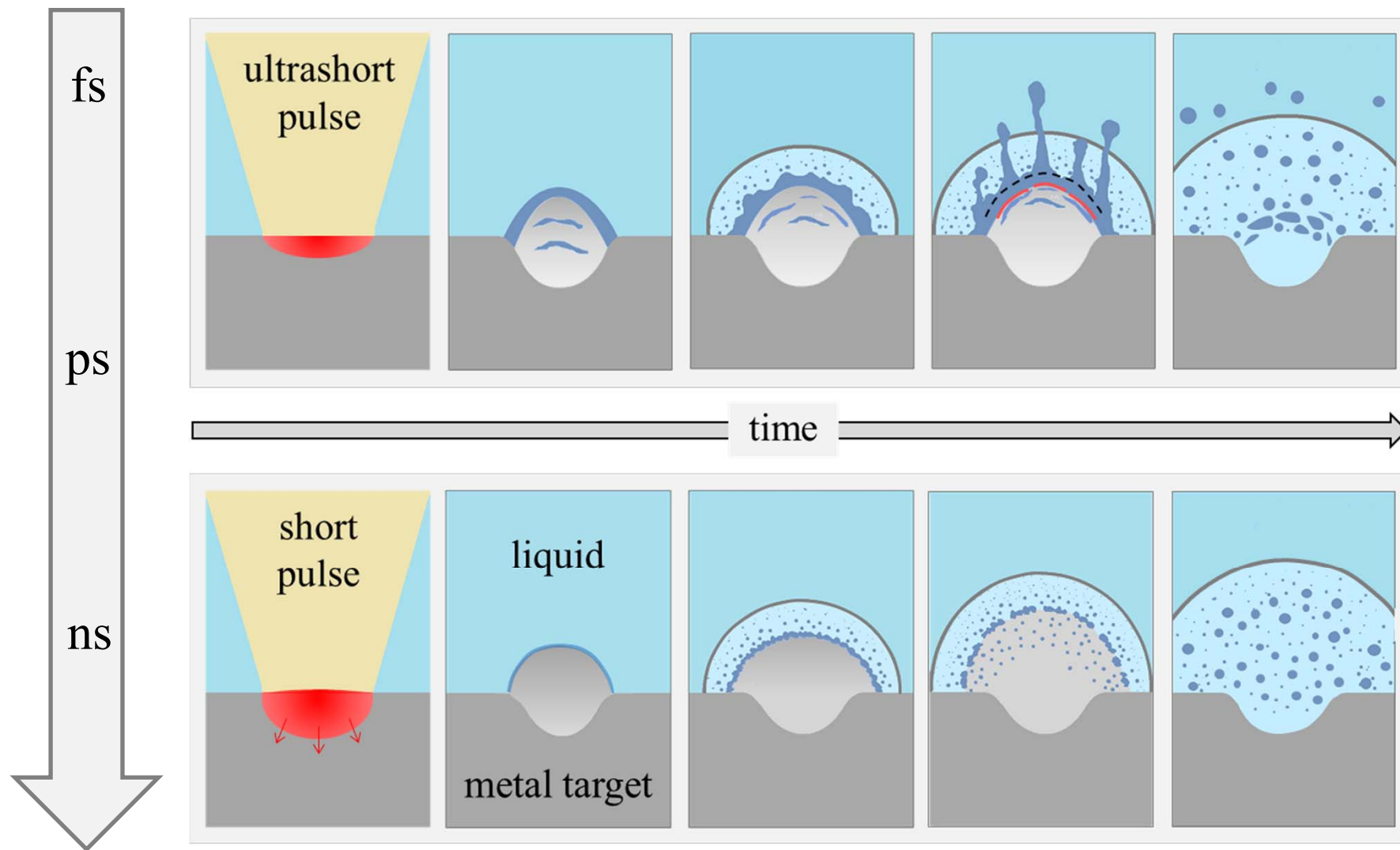
Shih *et al.*, *J. Phys. Chem. C* **121**, 16549, 2017

Shih *et al.*, *J. Colloid Interface Sci.* **489**, 3, 2017

Shugaev *et al.*, *Appl. Surf. Sci.* **417**, 54, 2017

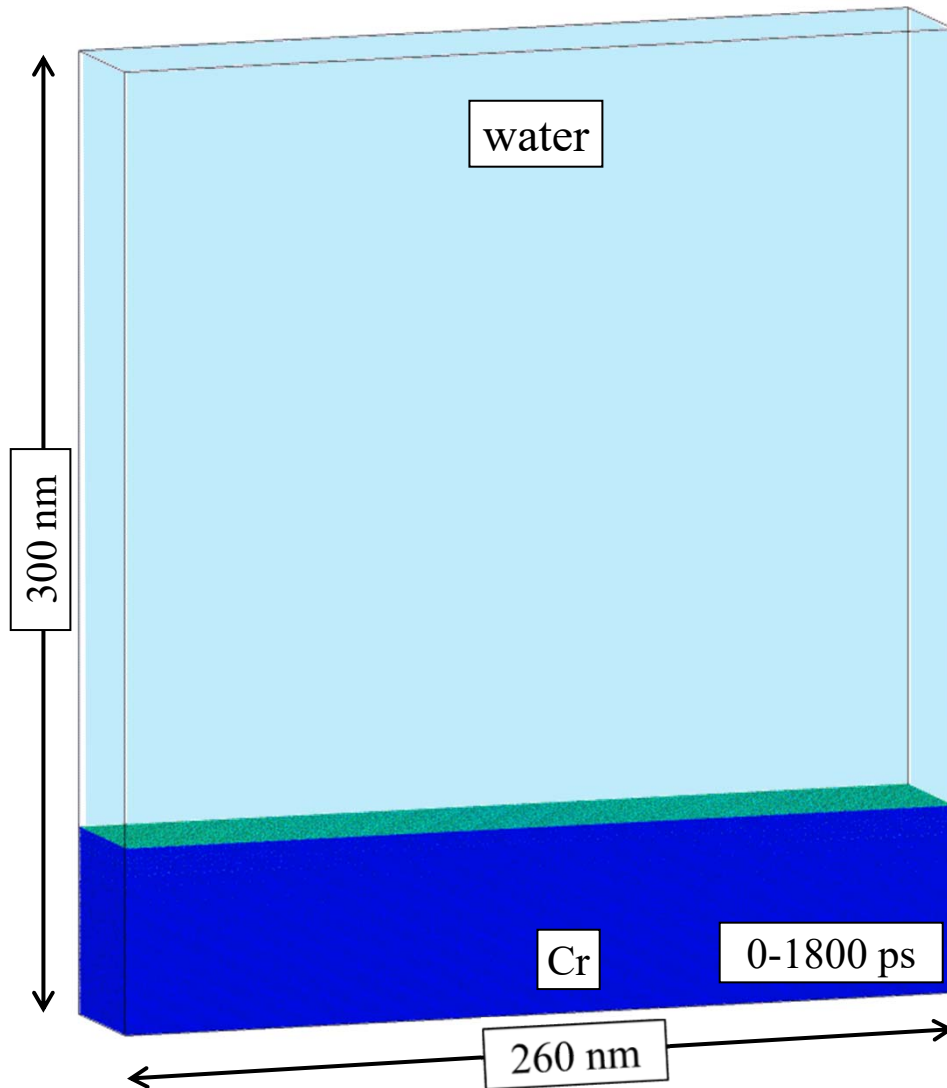
Shih *et al.*, *Nanoscale* **10**, 6900, 2018

The effect of pulse duration on nanoparticle generation in PLAL

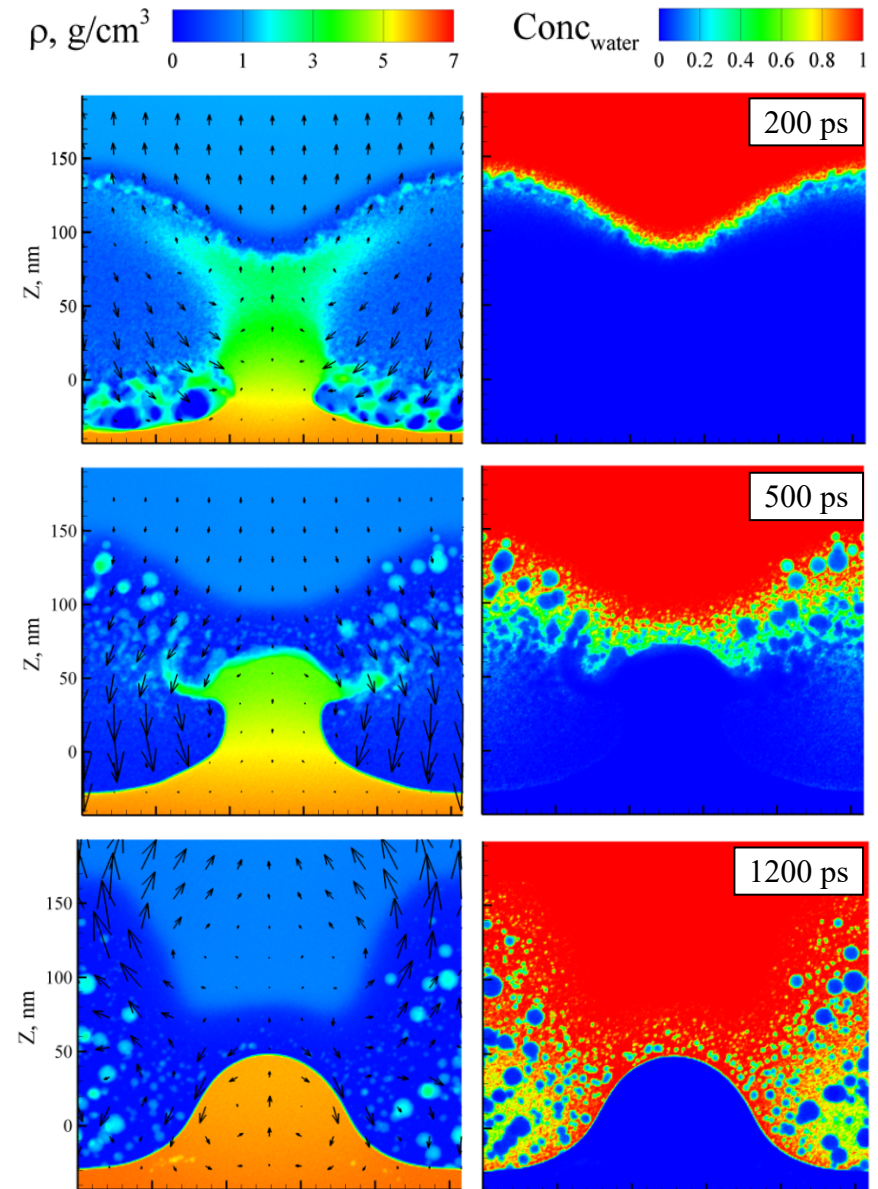


Shih *et al.*, *Phys. Chem. Chem. Phys.* **22**, 7077, 2020

Spatially modulated ablation in water



- Rapture of the transient metal layer
- Fast mixing and quenching

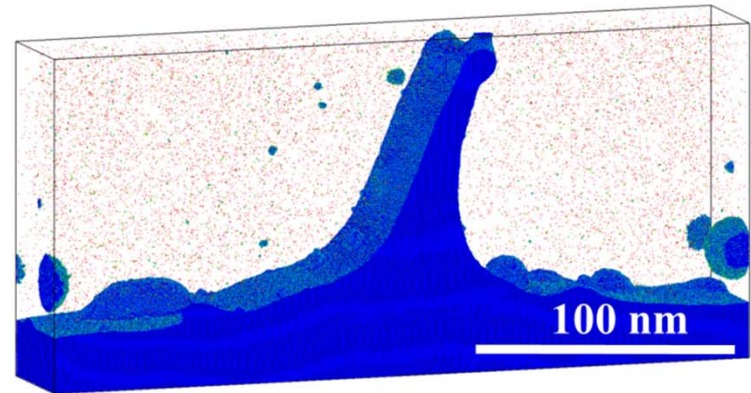
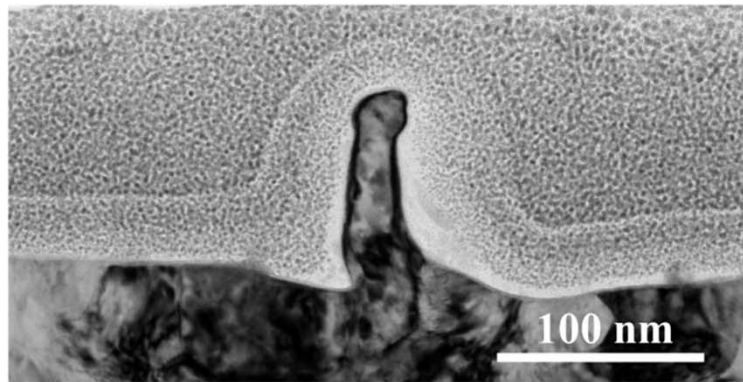


Shih *et al.*, *Nanoscale* **12**, 7674, 2020

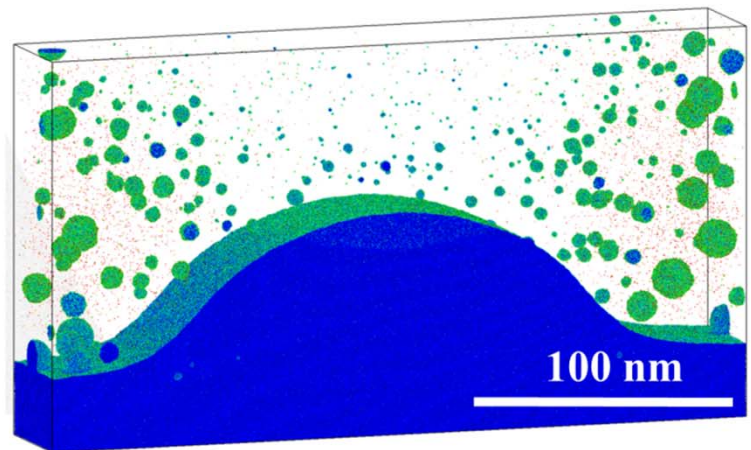
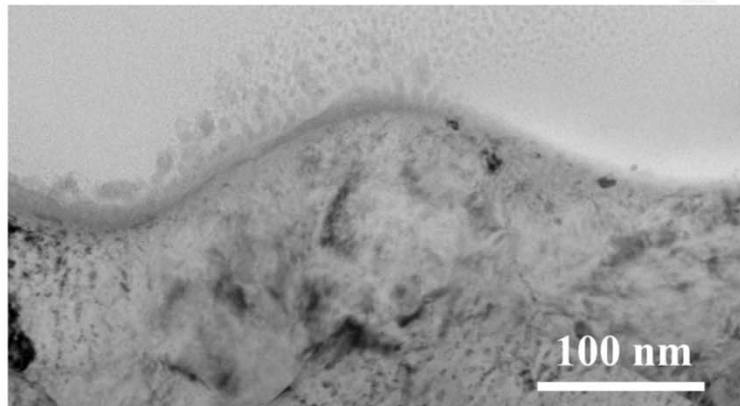
Effect of water environment on surface morphology

TEM images of ripple cross-sections and corresponding simulated surface structures

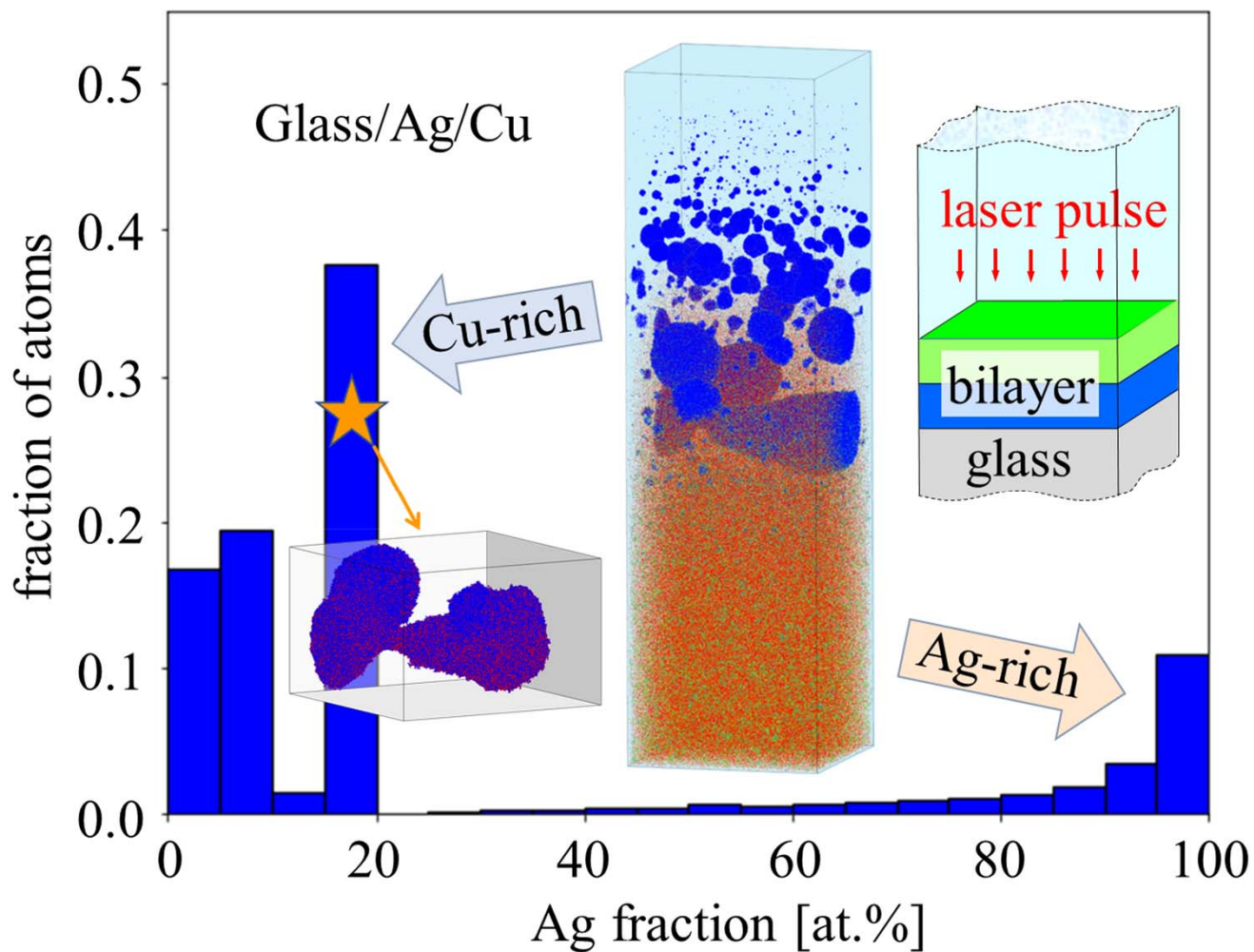
in air



in water



Laser ablation of AgCu bilayer thin films in water



Shih *et al.*, *J. Phys. Chem. C* **125**, 2132, 2021

Laser ablation of AgCu bilayer thin films in water

pressure-transmitting boundary conditions

coarse-grained MD representation of liquid environment (36.3 million CG particles)

Shih *et al.*, *J. Colloid Interface Sci.* **489**, 3, 2017.

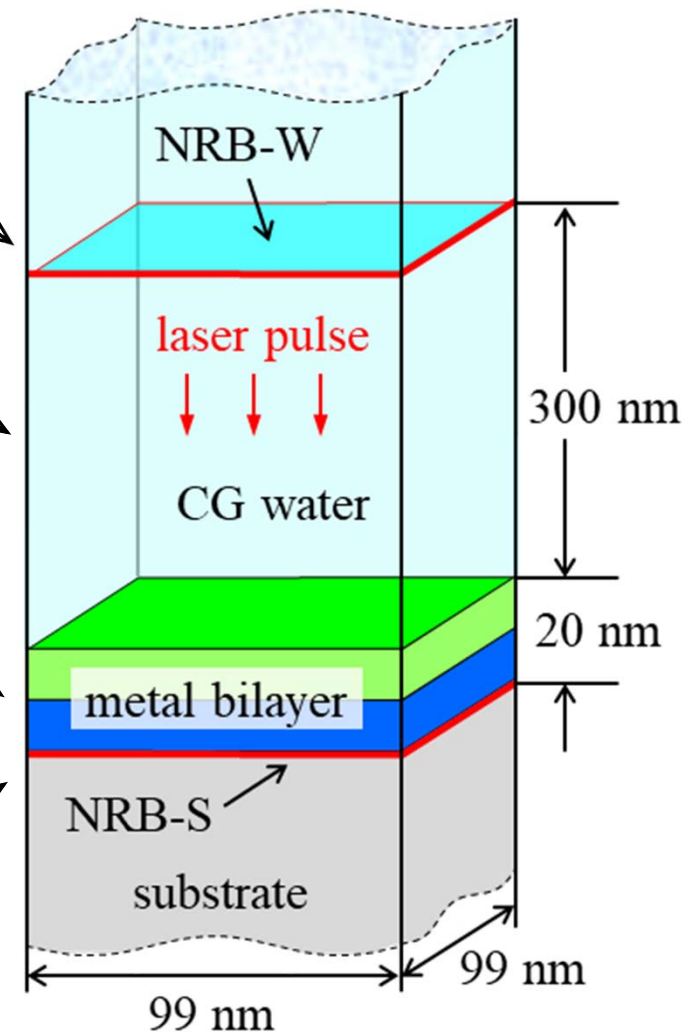
TTM-MD representation of metal bilayer

8.29 million Cu and 5.76 million Ag atoms

Embedded Atom Method (EAM) potential

Williams *et al.*, *Modelling Simul. Mater. Sci. Eng.* **14**, 817, 2006.

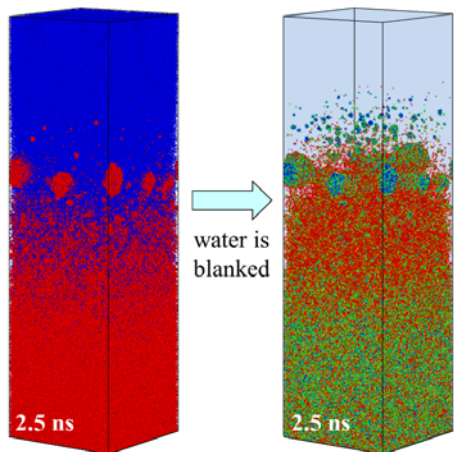
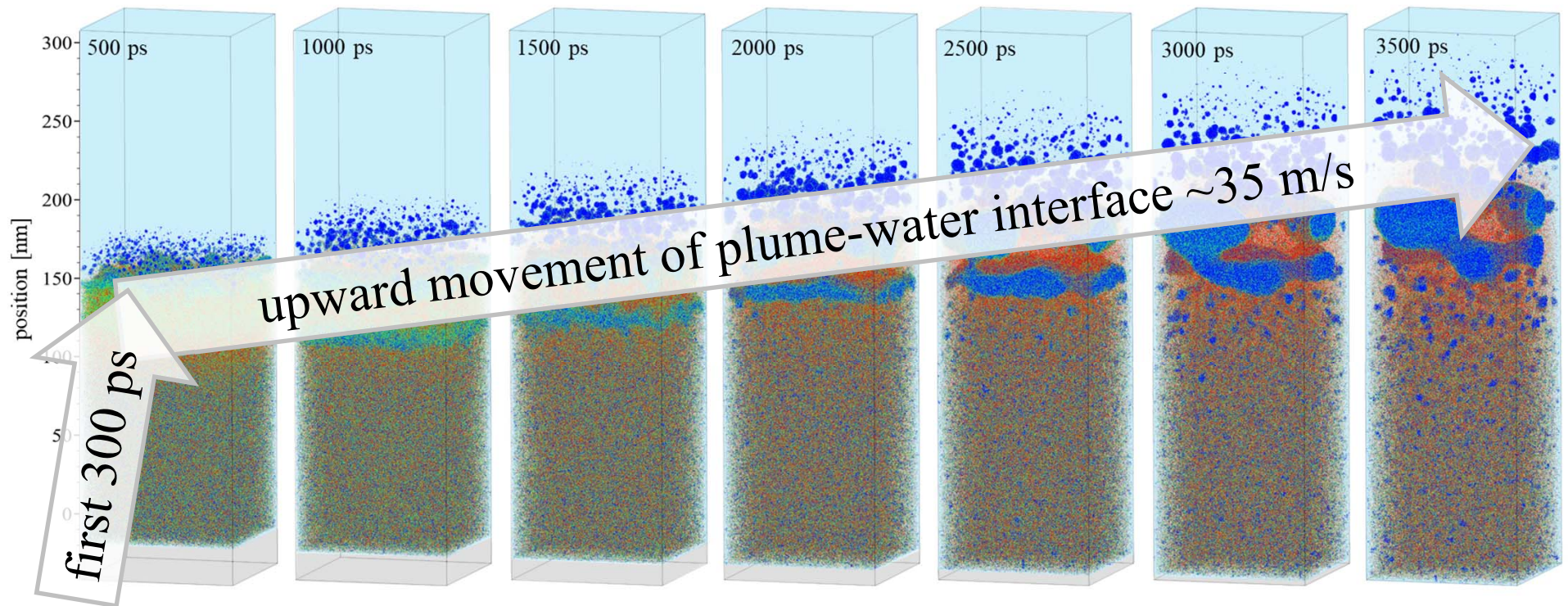
pressure-transmitting boundary conditions



$$\tau_L = 100 \text{ fs}, F_{abs} = 100 \text{ mJ/cm}^2, \lambda = 800 \text{ nm}$$

Shih *et al.*, *J. Phys. Chem. C* **125**, 2132, 2021

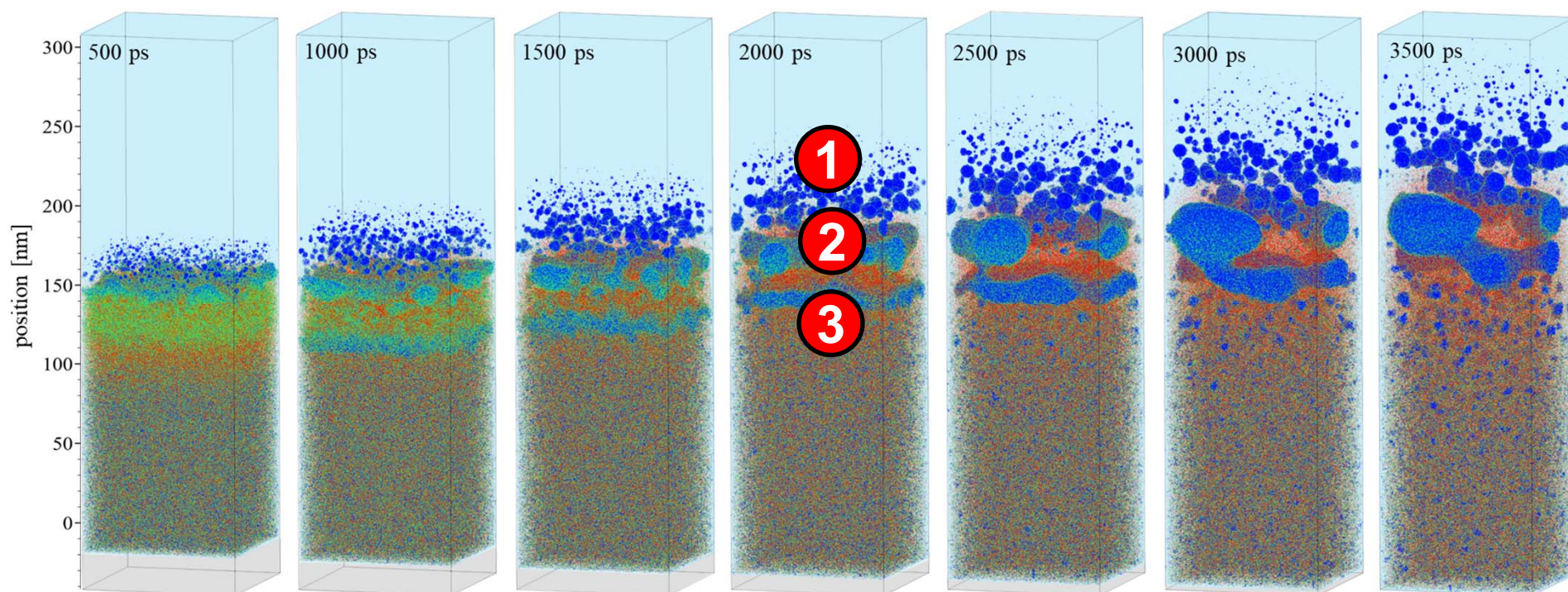
Laser ablation of glass/Cu/Ag bilayer in water



- Rapid deceleration of the ablation plume by water;
- Accumulation of the plume at the interface with water;
- Slower steady upward movement of the interface with a velocity of ~ 35 m/s.

- water is blanked to expose the processes occurring in ablation plume

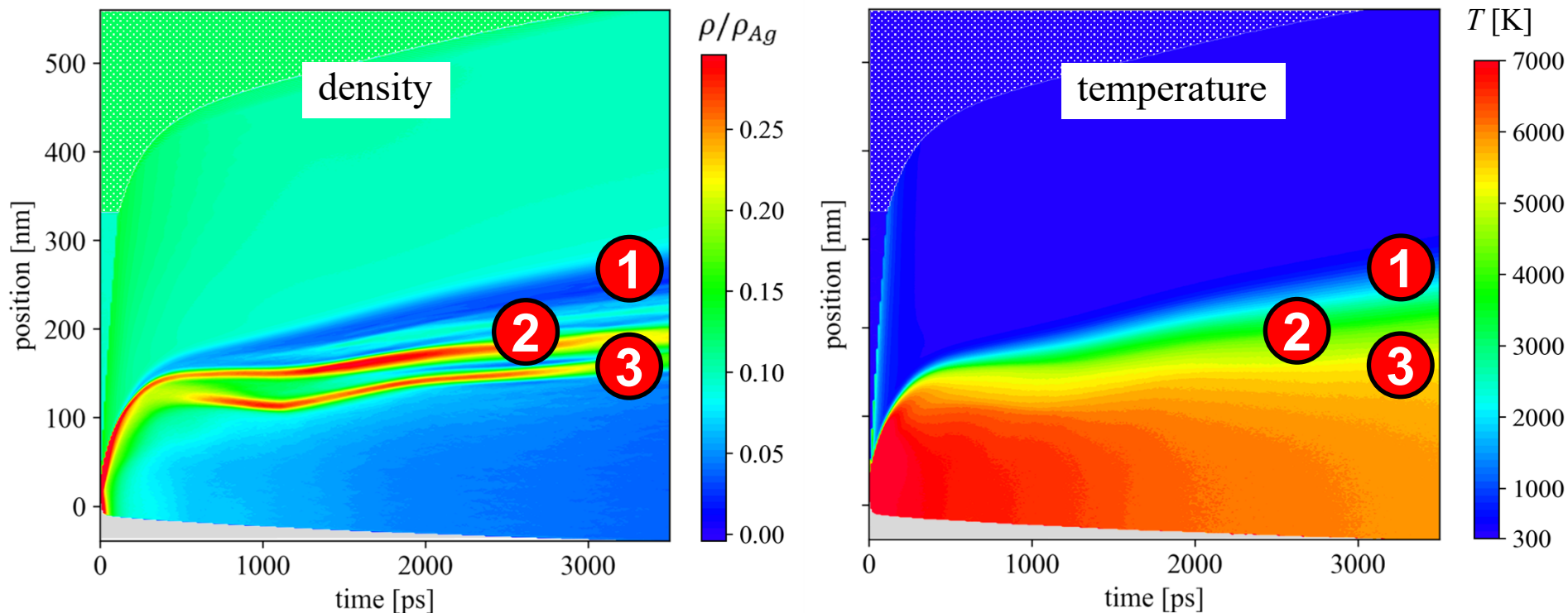
Laser ablation of glass/Cu/Ag bilayer in water



Stratification of the interfacial region into three parts:

1. top region of rapid nucleation and growth of numerous small nanoparticles,
2. complex coarse morphology of interconnected liquid regions,
3. continuous thin metal layer that retains its integrity up to ~ 2500 ps.

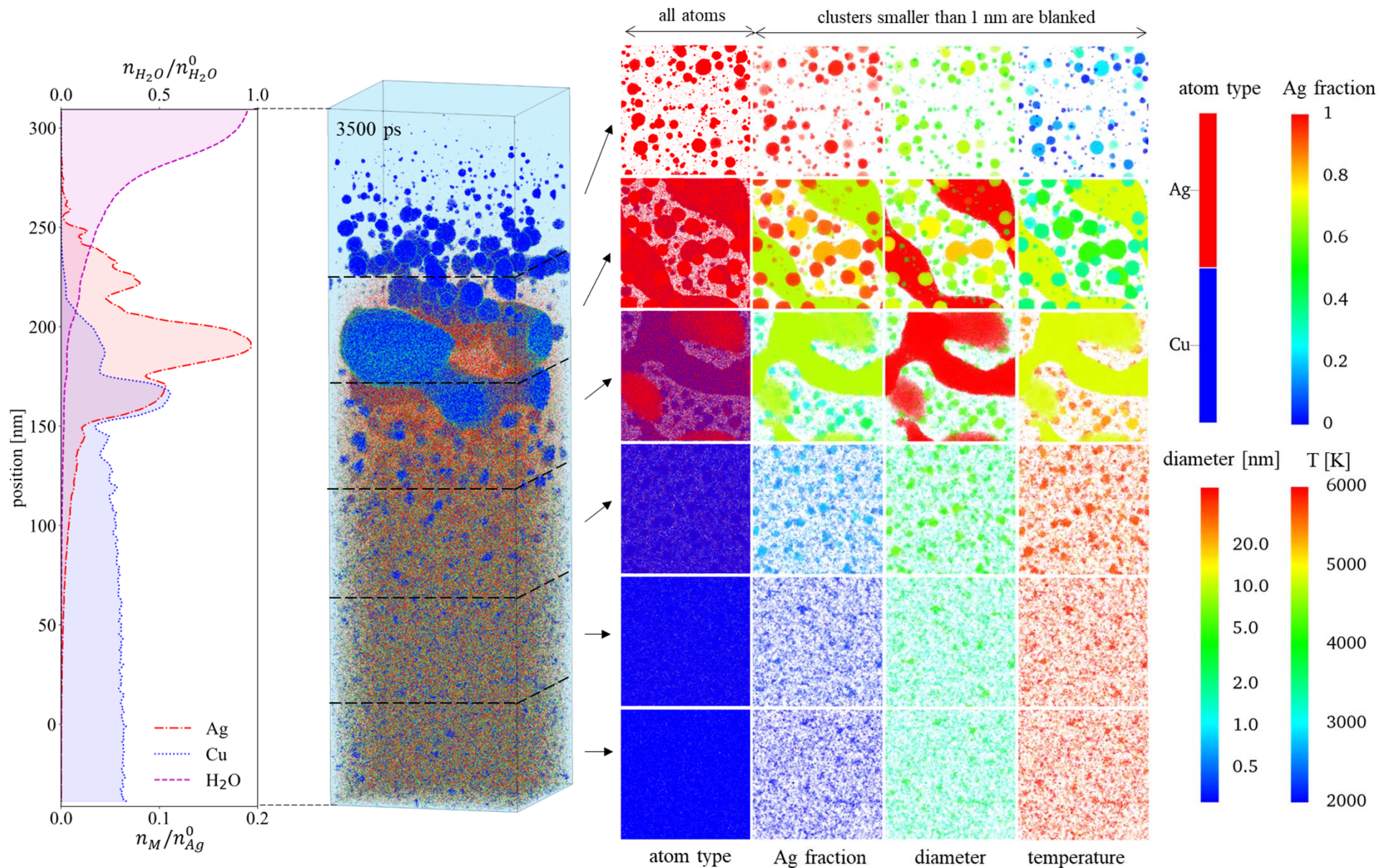
Laser ablation of glass/Cu/Ag bilayer in water



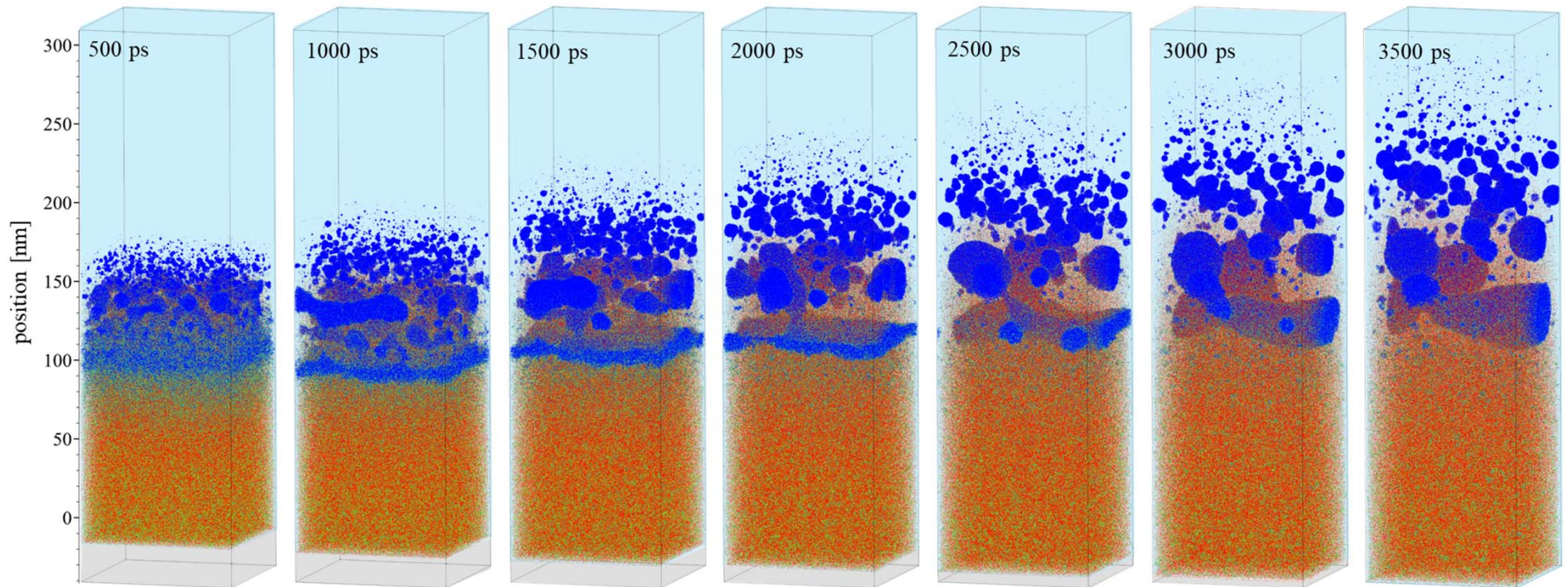
Stratification of the interfacial region into three parts:

1. top region of rapid nucleation and growth of numerous small nanoparticles,
2. complex coarse morphology of interconnected liquid regions,
3. continuous thin metal layer that retains its integrity up to ~ 2500 ps.

Laser ablation of glass/Cu/Ag bilayer in water



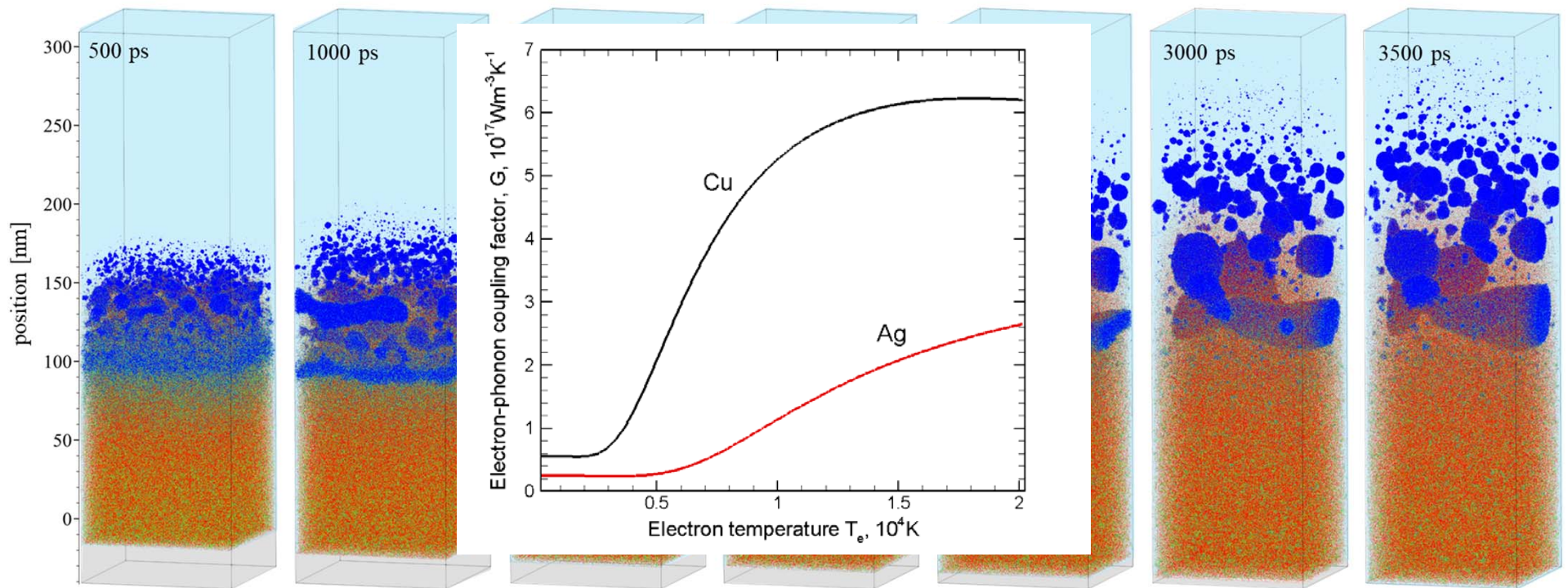
Laser ablation of glass/Ag/Cu bilayer in water



Same qualitative picture, but some quantitative differences related to $G_{Cu} > G_{Au}$:

1. less vigorous initial expansion,
2. lower T of the vapor in the bottom part of the system,
3. more numerous large (10s nm) droplets in the upper part of the interfacial region and smaller largest droplet at the lower part of the interfacial region.

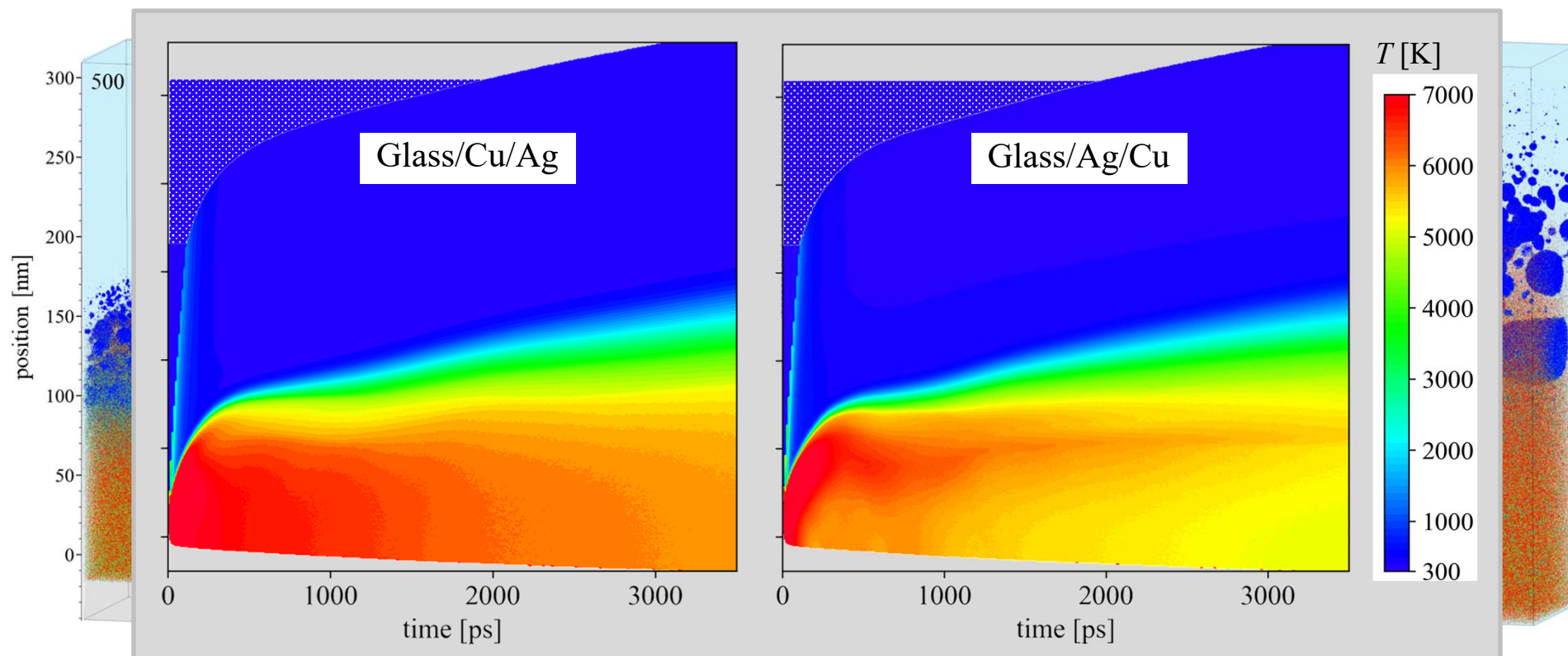
Laser ablation of glass/Ag/Cu bilayer in water



Same qualitative picture, but some quantitative differences related to $G_{Cu} > G_{Au}$:

1. less vigorous initial expansion,
2. lower T of the vapor in the bottom part of the system,
3. more numerous large (10s nm) droplets in the upper part of the interfacial region and smaller largest droplet at the lower part of the interfacial region.

Laser ablation of glass/Ag/Cu bilayer in water

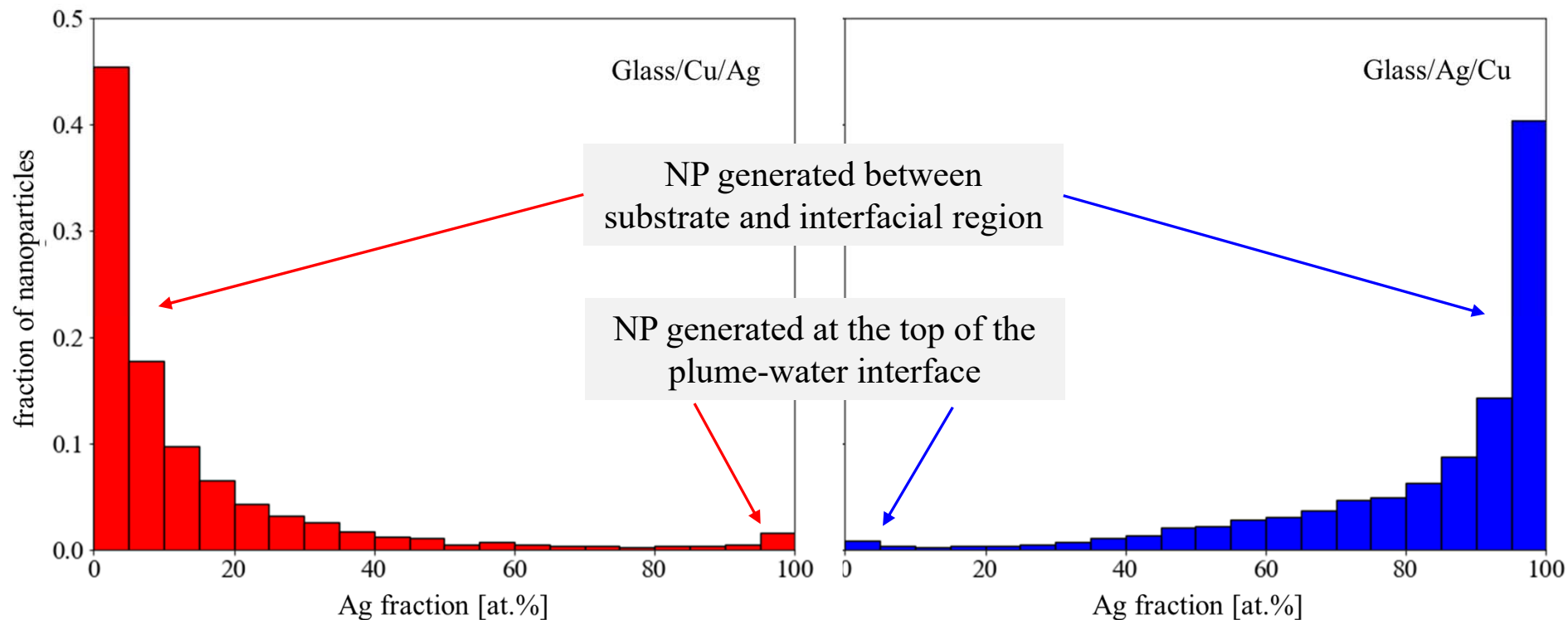


Same qualitative picture, but some quantitative differences related to $G_{Cu} > G_{Au}$:

1. less vigorous initial expansion,
2. lower T of the vapor in the bottom part of the system,
3. more numerous large (10s nm) droplets in the upper part of the interfacial region and smaller largest droplet at the lower part of the interfacial region.

Nanoparticle composition at 3.5 ns after the pulse

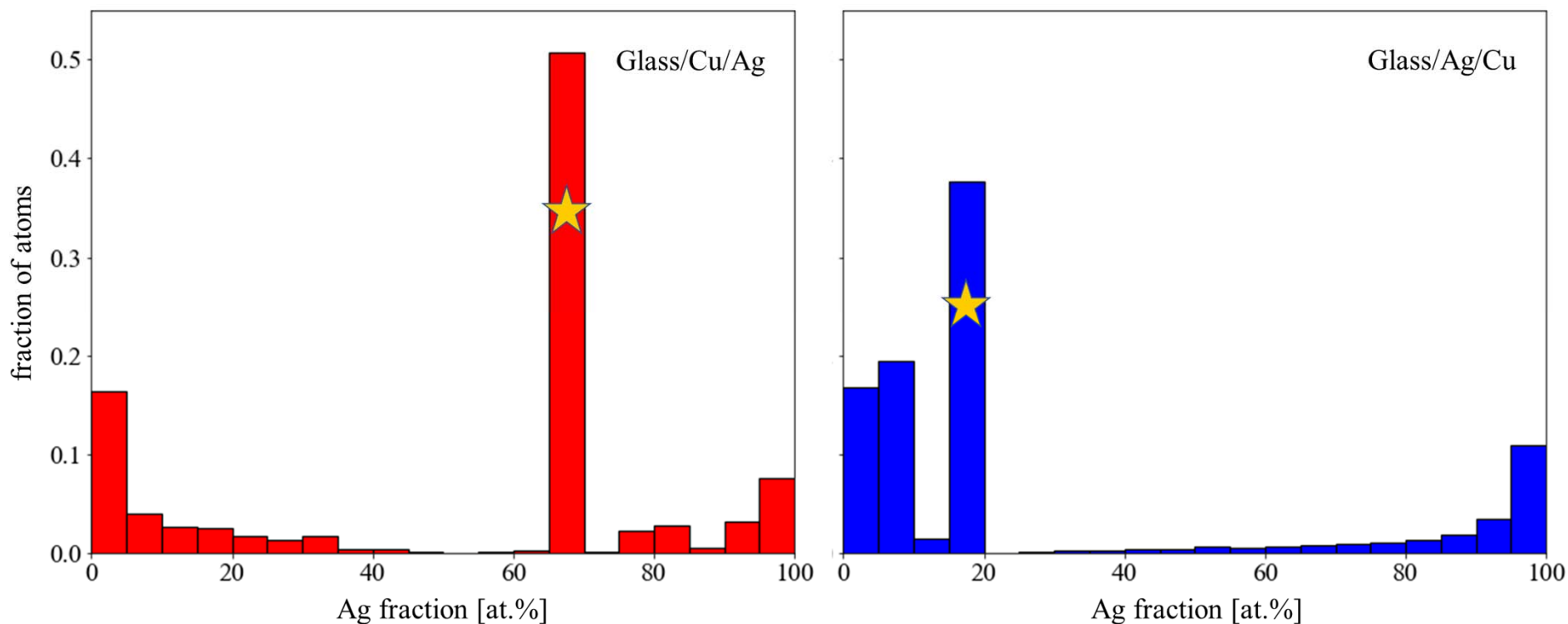
Number of NPs



- Limited mixing prior to the formation of the nanoparticles.
- Central parts of the distributions (correspond to well-mixed compositions) are depleted of nanoparticles.
- Limited mixing is surprising, since fluence is ~ 3 times the ablation threshold

Nanoparticle composition at 3.5 ns after the pulse

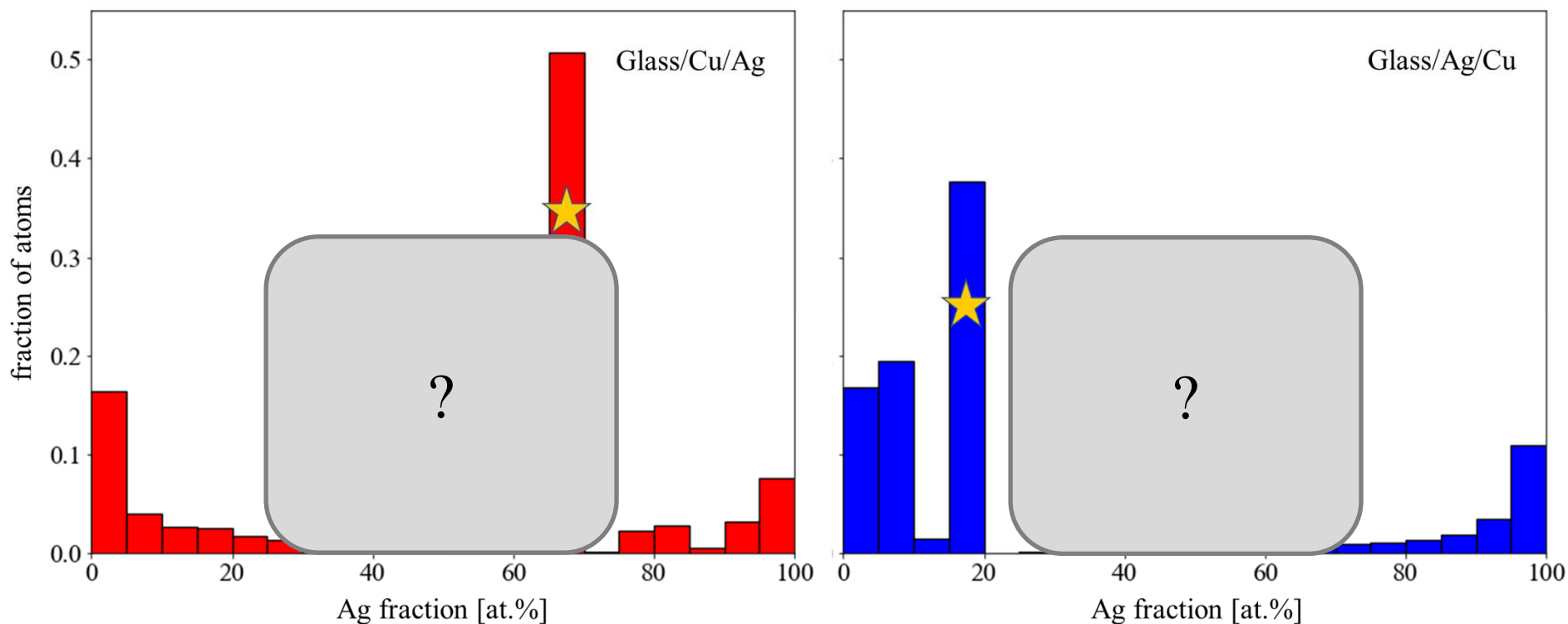
Number of atoms in NPs



- Limited mixing prior to the formation of the nanoparticles.
- Central parts of the distributions (correspond to well-mixed compositions) are depleted of nanoparticles.
- Limited mixing is surprising, since fluence is ~ 3 times the ablation threshold

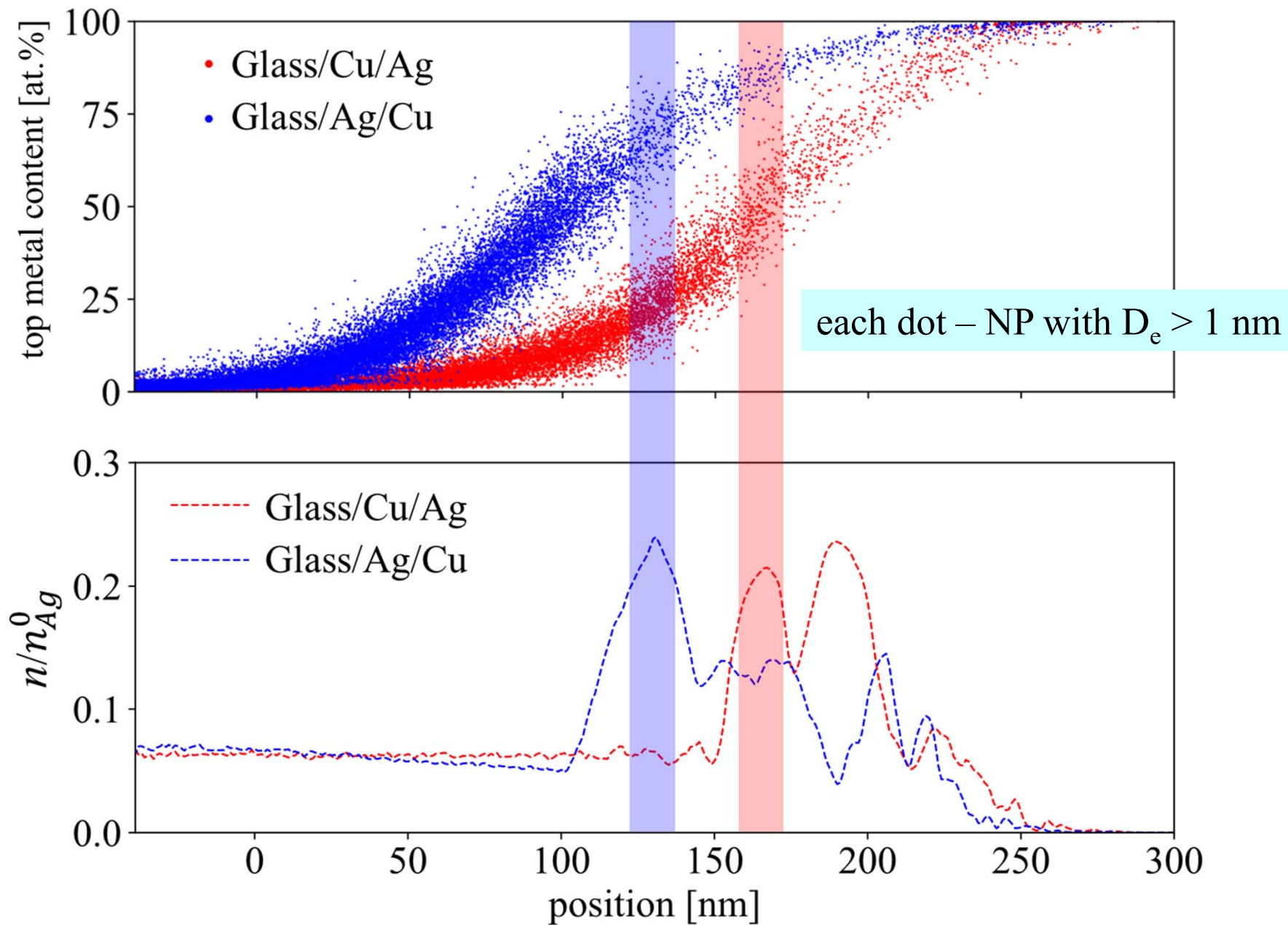
Nanoparticle composition at 3.5 ns after the pulse

Number of atoms in NPs



- Limited mixing prior to the formation of the nanoparticles.
- Central parts of the distributions (correspond to well-mixed compositions) are depleted of nanoparticles.
- Limited mixing is surprising, since fluence is ~ 3 times the ablation threshold

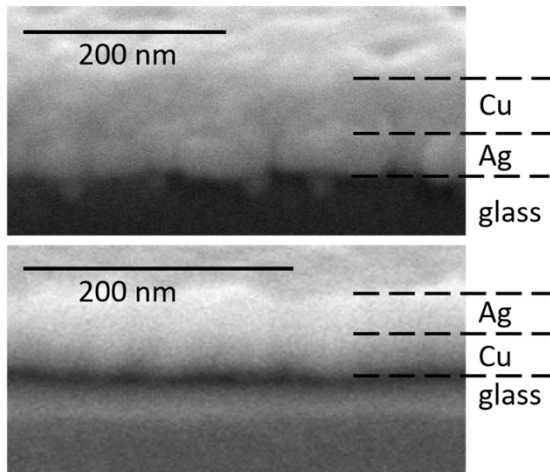
Nanoparticle composition at 3.5 ns after the pulse



Experimental verification

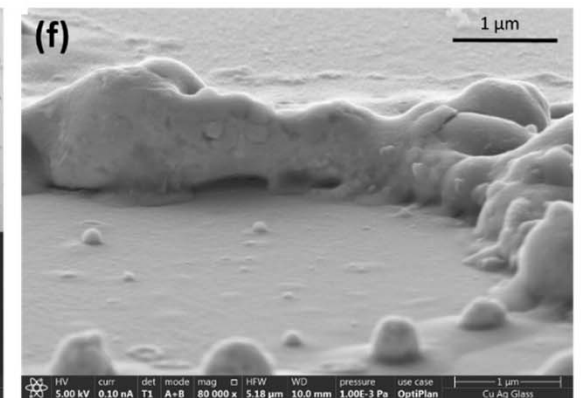
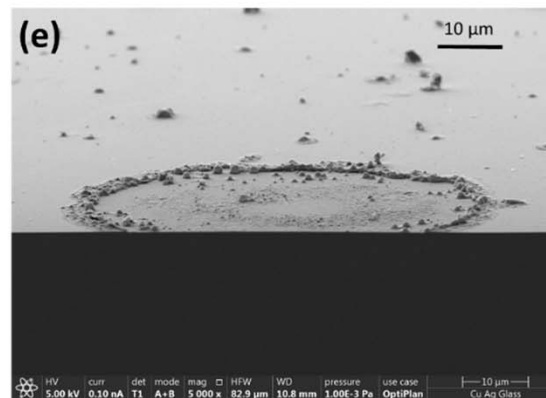
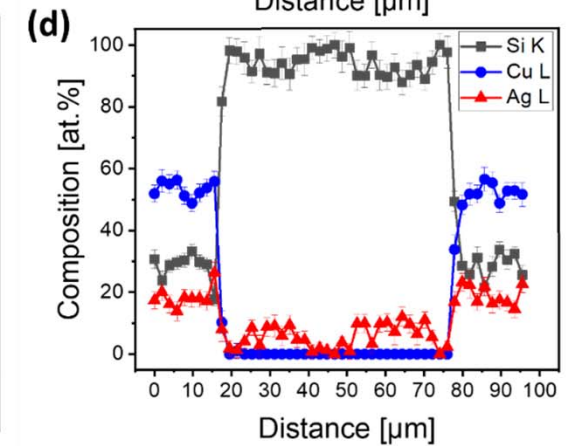
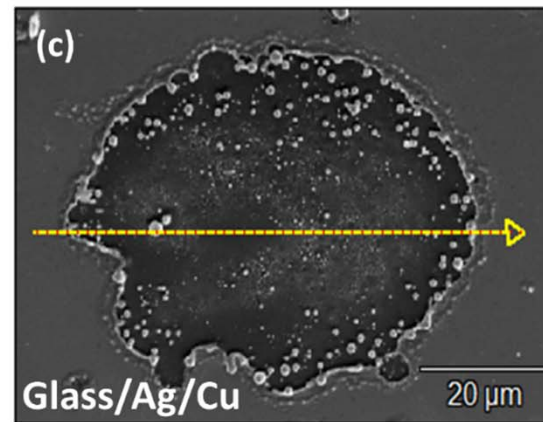
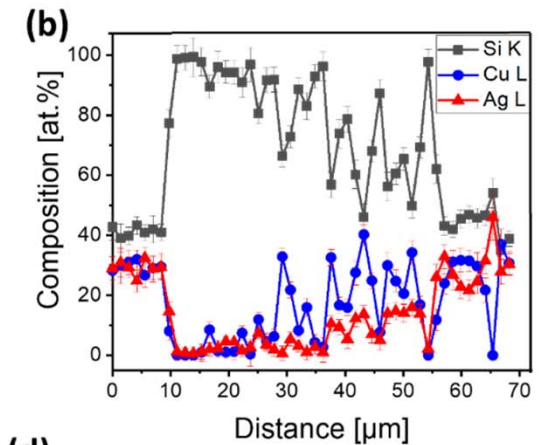
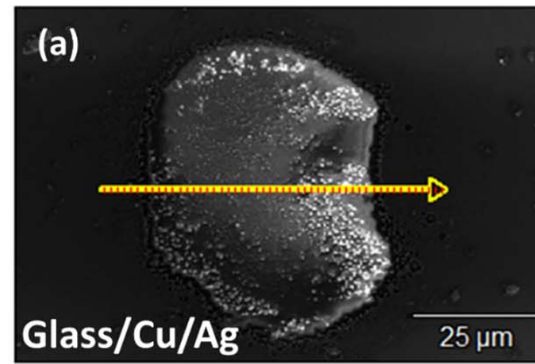
Christoph Rehbock
 Anna Tymoczko
 Ulf Wiedwald
 Marius Kamp
 Ulrich Schuermann
 Lorenz Kienle
 Stephan Barcikowski

University of Duisburg-Essen
 Kiel University

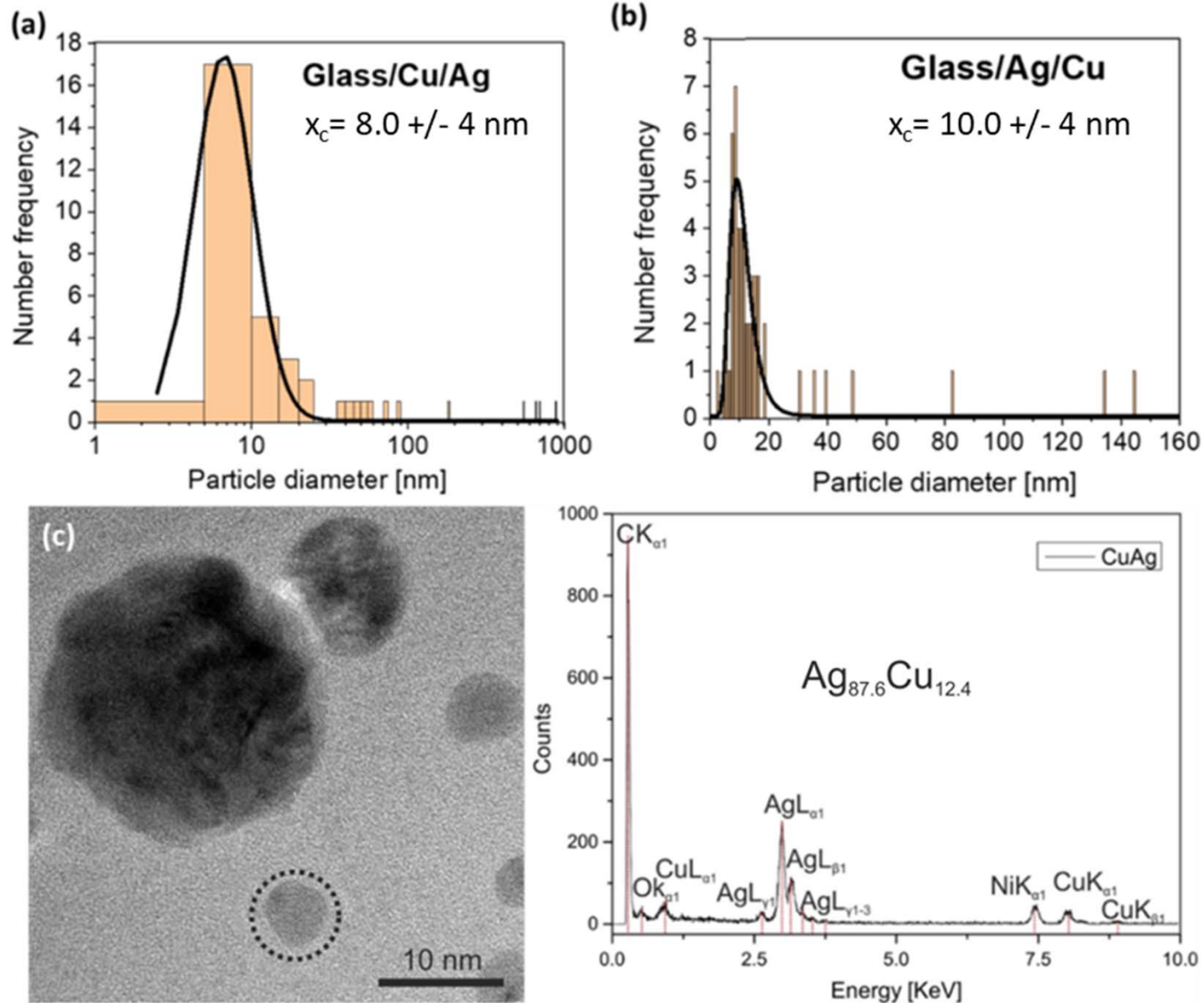


Glass/Cu/Ag
 39 nm Ag + 40 nm Cu

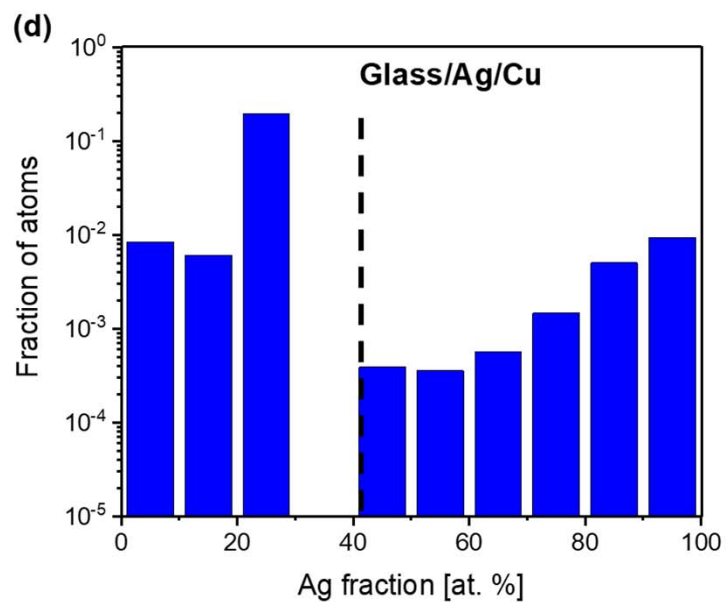
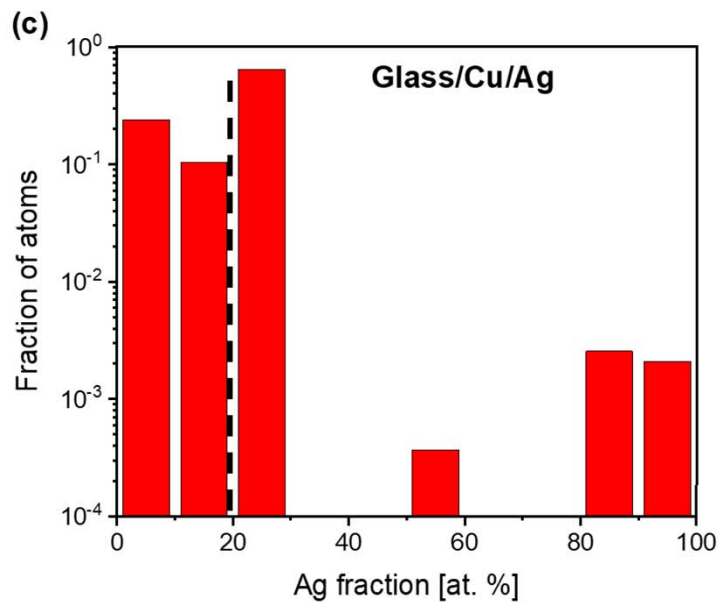
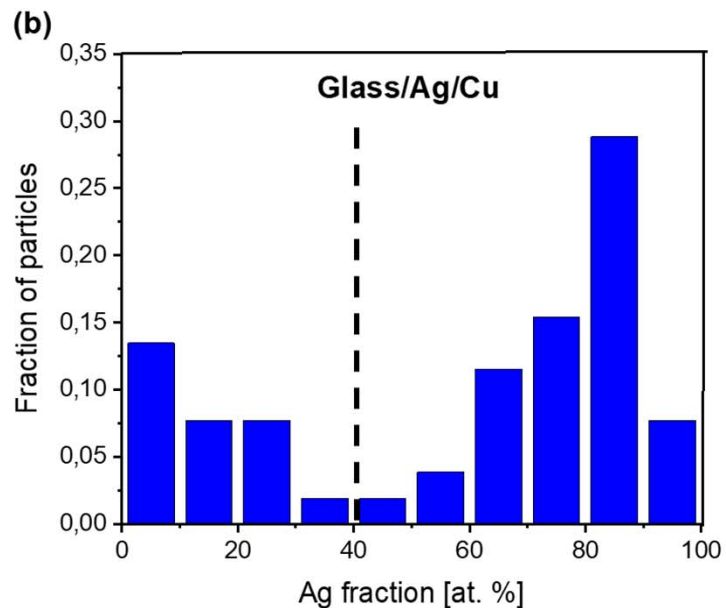
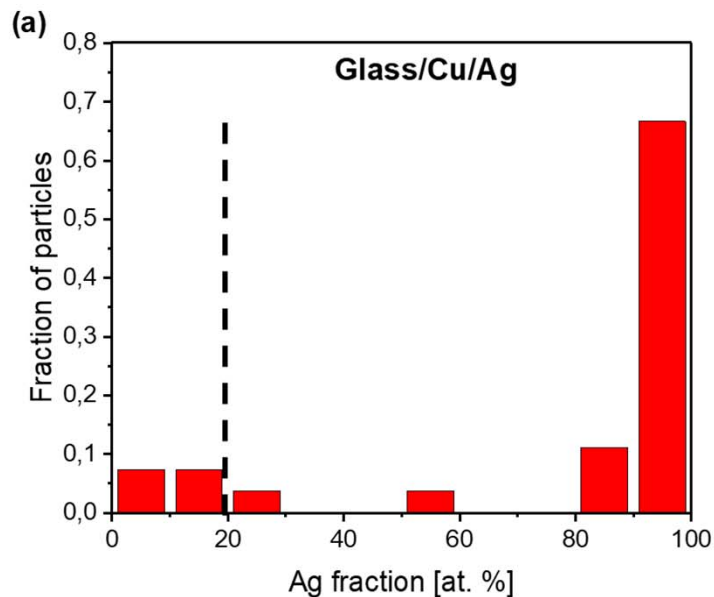
Glass/Ag/Cu
 65 nm Cu + 23 nm Ag



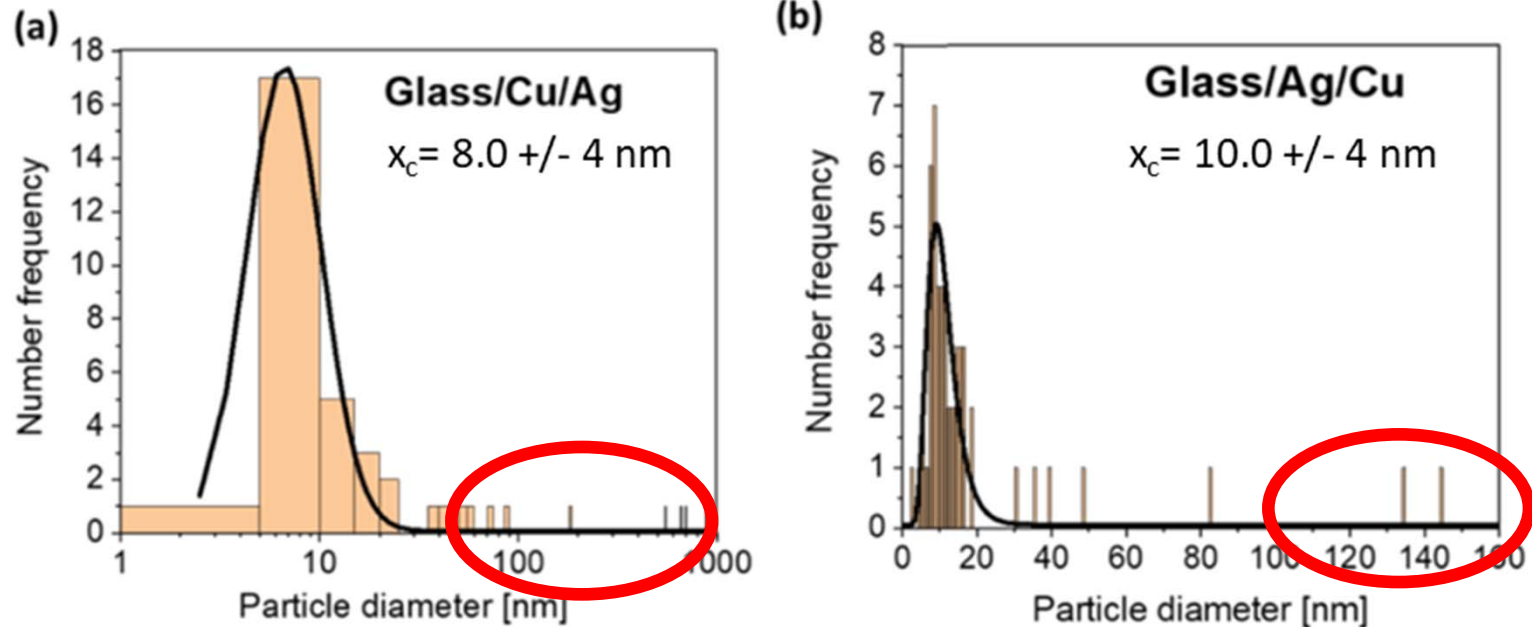
Experimental verification



Experimental verification

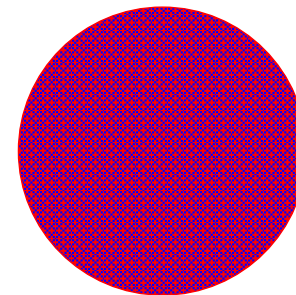
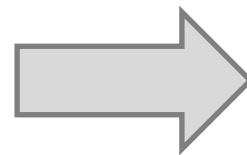


Nanoparticles larger than film thickness?



Diameters of the largest nanoparticles $>$ thickness of the original bilayer films.

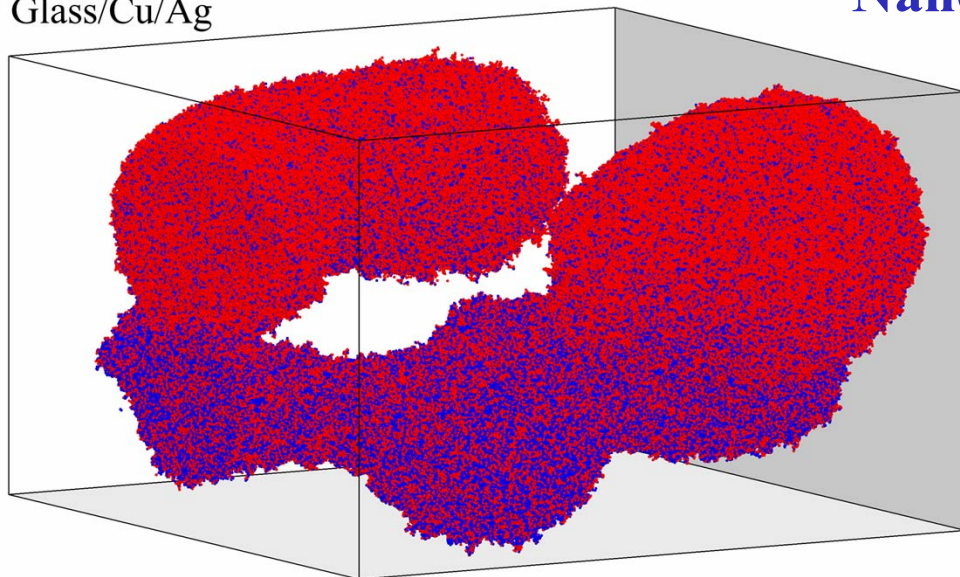
$3 \times$ (phase explosion threshold)



?

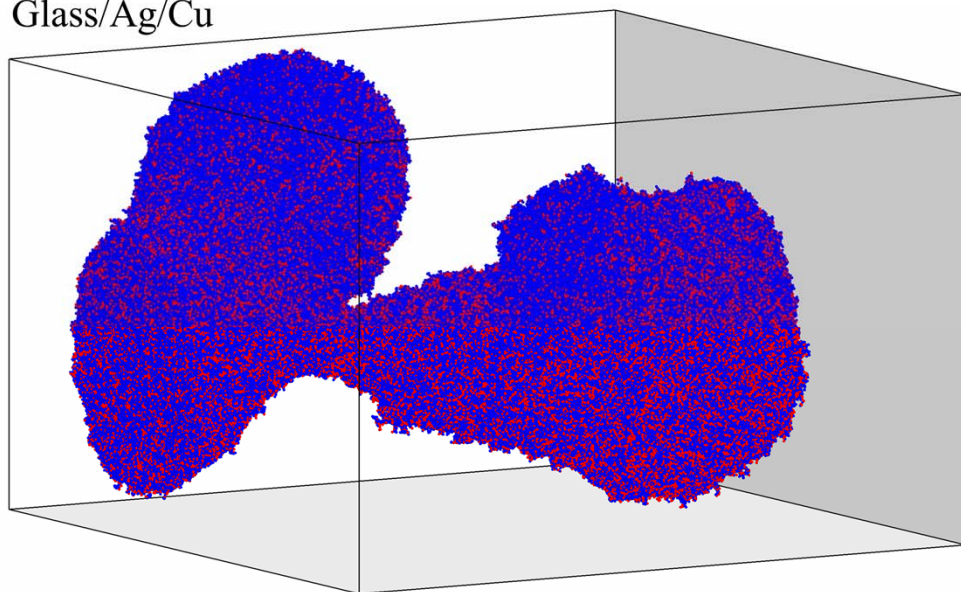
Nanoparticles larger than film thickness?

Glass/Cu/Ag



4,813,971 atoms, $D_e = 52.0$ nm, $C = 68$ at.% Ag

Glass/Ag/Cu



3,969,848 atoms, $D_e = 45.9$ nm, $C = 20$ at.% Ag

atom type

Ag

Cu

Accumulation of plume at the interface with water



Formation and decomposition of a transient liquid layer



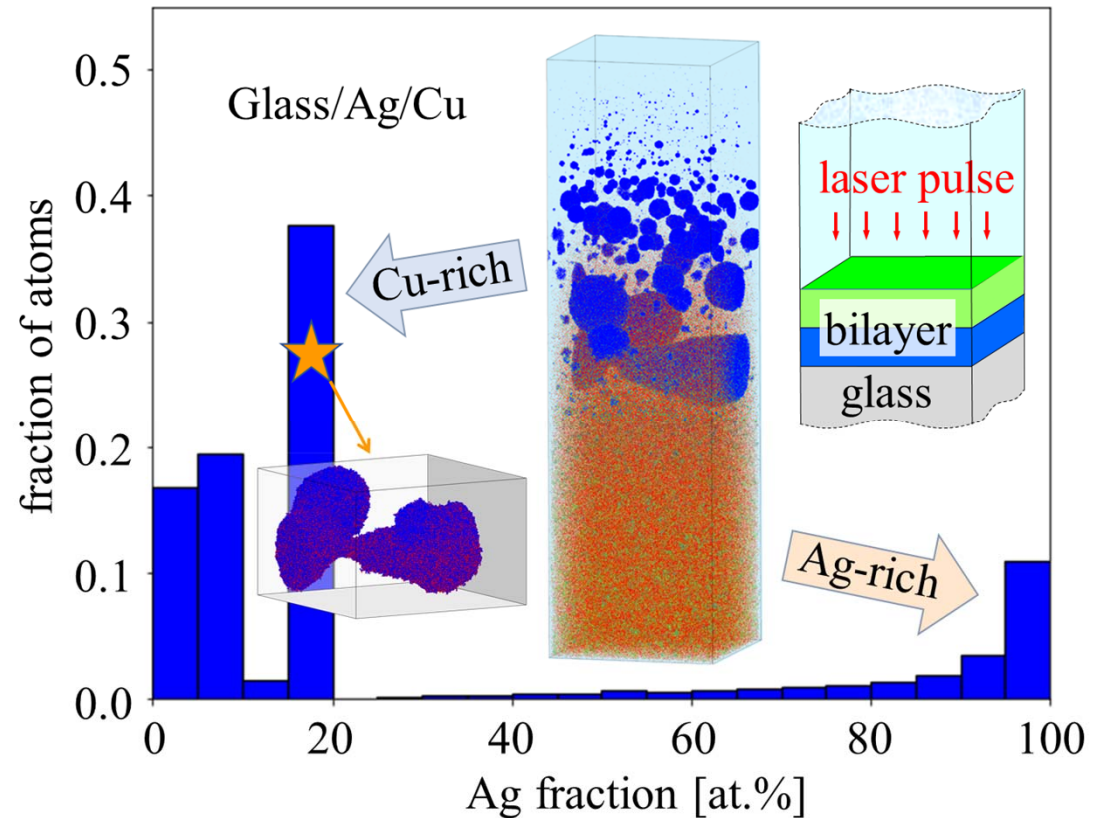
Nanoparticles more than twice larger than the thickness of the original bilayer films

Summary

Two surprising observations:

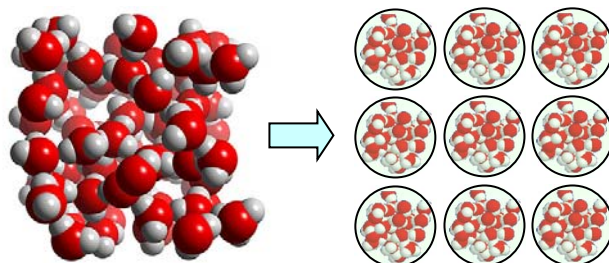
1. Nanoscale spatial separation of the two components in the bilayer leads to a sharp departure from the complete quantitative mixing in the colloidal nanoparticles.

2. The largest nanoparticles can exceed the thickness of the film.



Explained by complex dynamic interaction between the ablation plume and liquid environment: Accumulation of plume at the interface with liquid → formation and decomposition of a hot liquid layer that prevents mixing and yields large nanoparticles

Coarse-grained MD representation of liquid environment



Heat bath approach accounts for missing internal degrees of freedom

Tabetah *et al.*, *J. Phys. Chem. B* **118**, 13290, 2014; Shih *et al.*, *J. Colloid Interface Sci.* **489**, 3, 2017

properties of water	experiment	CG model	Δ , %
density, ρ , g/cm ³	1.0	1.0	0
heat capacity, c_p , J/(kg K)	4.2×10^3	4.2×10^3	0
bulk modulus, K , GPa	2.2	1.8	18
speed of sound, c_s , m/s	1483	1342	9
melting temperature, T_m , K	273	330	21
critical temperature, T_c , K	647	520	20
critical density, ρ_c , g/cm ³	0.322	0.398	24
viscosity, η , cP	0.894	0.910	2
surface energy, σ , J/m ²	0.072	0.073	1

**7th Venice International School on
Lasers in Materials Science - SLIMS**

July 10-18, 2022

Isola di San Servolo, Venice, Italy

<http://www.slims.polimi.it/>



**Symposium on Computer Modeling of Laser
and Ion Beam Interactions with Materials**

at the 10th International Conference on
Multiscale Materials Modeling, Baltimore,
Maryland (November 7-11, 2021)

<https://mmm10.jhu.edu/symposia/Computer-modeling-of-laser-and.html>